Continuum and discrete models for unbalanced woven fabrics

Angela Madeo, Gabriele Barbagallo, Marco Valerio d'Agostino, Philippe Boisse

Continuum and discrete models for unbalanced woven fabrics

Angela Madeo*†, Gabriele Barbagallo‡, Marco Valerio D'Agostino§and Philippe Boisse¶

March 3, 2017

Abstract

The classical models used for describing the mechanical behavior of woven fabrics do not fully account for the whole set of phenomena that occur during the testing of such materials. This lack of precision is mainly due to the absence of energy terms related to the microstructural properties of the fabric and, in particular, to the bending stiffness of the yarns. The importance of the bending stiffness on the overall mechanical behavior of woven reinforcements, if already essential for the complete description of balanced fabrics, becomes even more important in the case of unbalanced ones. In this paper it is shown that the unbalance in the bending stiffnesses of the warp and weft yarns produces macroscopic effects that are extremely visible: we mention, for example, the asymmetric S-shape of a woven interlock subjected to a Bias Extension Test (BET).

We propose to introduce a constrained micromorphic model and, simultaneously, a discrete model that are both able to account for i) the angle variation between warp and weft tows, ii) the unbalance in the bending stiffness of the yarns and iii) the relative slipping of the tows.

The introduced constrained micromorphic model is rigorously framed in the spirit of the Principle of Virtual Work for the study of the equilibrium of continuum bodies. A suitable constraint is introduced in such micromorphic model by means of Lagrange multipliers in the strain energy density and the resulting constrained model is seen to tend to a particular second gradient one. The main advantage of using such constrained micromorphic model is that the kinematical and traction boundary conditions that can be imposed on some sub-portions of the boundary of the considered body take a natural and unique meaning.

The discrete model is set up by opportunely interconnecting Euler-Bernoulli beams with different bending stiffnesses in the two directions by means of rotational and translational elastic springs. The main advantage of such discrete model is that the slipping of the tows is described in a rather realistic way. Suitable numerical simulations are presented for both the continuum and the discrete models and a comparison between the simulations and the experimental results is made showing a definitely good agreement.

Introduction

For decades textile composites made of woven fabrics have been successfully employed in aircraft and automobile engineering and they are gaining an even increased interest due to their excellent mechanical properties such as a very high specific-strength and excellent formability properties. Fibrous composite reinforcements present improved characteristics, namely high specific stiffness and strength, good deformability, dimensional stability, low thermal expansion, good corrosion resistance and many others. Among the quoted characteristics, the good deformability is what makes these materials perfect to be formed in various shapes with limited expenses. On the other hand, some complex behaviors of the woven fabrics, for instance the onset of wrinkling and slippage, limit the admissible deformations during the stamping operations and can render the modeling of such materials difficult to be achieved. Due to the complexity of the micro-macro behavior of fibrous composite reinforcements, the need of a comprehensive model for the prediction of the mechanical response of such materials during the forming represents a real scientific challenge (see e.g. [9]).

The structure of the fabric is characterized by two main directions of woven tows (warp and weft) and, therefore, in those directions the fabric has a very high extensional rigidity. The way in which these fabrics

*angela.madeo@insa-lyon.fr, LGCIE, Université de Lyon, INSA, 20 avenue Albert Einstein, 69621, Villeurbanne cedex, France

†Corresponding author

‡gabriele.barbagallo@insa-lyon.fr, LaMCoS, Université de Lyon, INSA, 20 avenue Albert Einstein, 69621, Villeurbanne cedex

§marco-valerio.dagostino@insa-lyon.fr, LaMCoS, Université de Lyon, INSA, 20 avenue Albert Einstein, 69621, Villeurbanne cedex

¶philippe.boisse@insa-lyon.fr, LaMCoS, Université de Lyon, INSA, 20 avenue Albert Einstein, 69621, Villeurbanne cedex

are weaved varies according to the different production methods and it is therefore possible to observe various schemes of weaving patterns such as those shown in figure 1 for unbalanced fabrics. Each of these schemes leads to a different type of composite reinforcements and thus to different mechanical properties. Furthermore, the warp and weft of a fabric can be either balanced (with the same properties) or unbalanced (the warp and weft present different characteristics due, for example, to a different number of constituting fibers). Such unbalanced fabrics may be of use, for example, in all those engineering applications that require a material that has to be stressed in a main direction. In such situations the use of an unbalanced fabric conveys a real advantage in terms of material response and therefore an economic advantage as well.

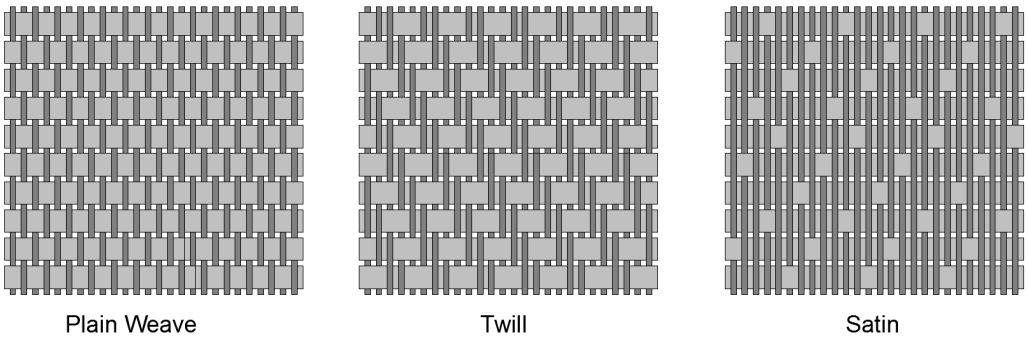

Figure 1: Schemes of weaving for unbalanced fibrous composite reinforcements

In order to produce the fabrics, the yarns (that are themselves composed of thousands of small carbon fibers) are weaved together forming a very complex texture. In such a structure it is no wonder that the interaction between the yarns and their behavior at a mesoscale play a fundamental role on the overall response of the material. One of the main features that determines the properties of the fabric is the friction between the yarns that both prevents the slipping and generates the shear rigidity of the fabric. This shear stiffness fundamentally determines the behavior of the fabric being usually orders of magnitudes lower than the elongation stiffness of the yarns. The shear angle variation between warp and weft can hence be thought to be the principal deformation mode of fibrous composite reinforcements. However, the shear stiffness of the fabric and the elongation stiffness of the yarns are not enough to fully describe the response of such materials. The yarns, possess an in-plane bending stiffness that determines some peculiar behaviors of the material at the macroscopic scale (see e.g. [26, 31]). Particularly, in the case of an unbalanced fabric the difference in the thickness of the two families of yarns leads to peculiar responses.

Notwithstanding the importance of a complete and effective modeling of fibrous composite reinforcements, the most common models for the description of the mechanical behavior of such materials fail to describe comprehensively their response.

In this paper we propose to use a micromorphic model to describe the mechanical behavior of unbalanced fibrous composite reinforcements with an application to the Bias Extension Test, which is a very well known mechanical test in the field of composite materials manufacturing (see e.g. [10, 39, 47, 68]).

We try to limit at most the complexity of such model by introducing a unique kinematical scalar field φ in addition to the classical macroscopic displacement u. As usual in micromorphic models, the strain energy density of the considered material is supposed to depend on the first gradients of both u and φ.

In order to describe at best the physics of the problem it is useful to interpret the variable φ as the angle variation between warp and weft, so that a dependence of the strain energy density on $\nabla\varphi$ actually accounts for the bending stiffness of the yarns. Indeed, it is possible to understand that when varying the angle from one value to a different one, this cannot be done too sharply, but a smooth gradient of the angle variation must occur that is physically associated to the bending of the tows.

As a matter of fact, the angle variation between the two material directions m_1 and m_2 can be directly associated to the gradient of the displacement field (such angle variation is known to be the invariant $i_8 = \langle m_1, C \cdot m_2 \rangle$, of the Cauchy-Green strain tensor C). In order to let the micromorphic variable φ tend to the angle variation i_8, we decide to use suitable Lagrange multipliers in the micromorphic strain energy density. The resulting constrained micromorphic model can be actually interpreted as a particular second gradient model since the first gradient of φ tends to the gradient of i_8 which is itself a function of the gradient of u.

As we will show in detail in the body of the paper, the proposed constrained micromorphic model is able to account for

- the basic mechanism of angle variation between warp and weft
- different bending rigidities in the warp and weft directions
- the decrimping and eventual relative slipping of the yarns.

When applying such constrained micromorphic model to the description of the Bias Extension Test (BET) on an unbalanced fabric, we are able to recover the characteristic macroscopic asymmetric S-shape of the specimen (essentially due to the two different bending stiffnesses), as well as the deformation patterns of warp and weft tows at the mesoscopic scale. More precisely, for what concerns the slipping of the yarns which is experimentally observed, it is accounted for in our continuum model by means of the introduction of "equivalent elongations" in the two material directions.

The reader may think that the fact of passing through a constrained micromorphic model to formulate a specific second gradient one is an artificial procedure that provides additional complexity to the modeling of the considered materials. Nevertheless, we will show that the fact of starting from a micromorphic model and to subsequently constrain it in order to tend to a second gradient one, is a more natural way to clarify the physical meaning of the considered problem. In particular, the fact of considering a micromorphic model avoids any confusion concerning the boundary conditions that can be imposed in the considered physical problem. We will see that we will be naturally led to impose kinematical boundary conditions that immediately take the precise physical meaning of imposing the displacement and the angle between warp and weft on given subsets of the boundary. Similarly, there will be a unique way to impose forces and double forces at the boundary of the considered micromorphic medium where tractions are assigned, and the introduced "force" will be seen to be directly related to the force which is measured by the employed testing machine.

On the other hand, if we would have started directly from a second gradient model the way of imposing physical boundary conditions would have been much more complicated. In fact, it is known (see e.g. [50, 54, 55]) that there is no a unique way to define forces and double forces in second gradient theories, but multiple combinations of such contact actions may be prescribed on the boundary which are all equally legitimate but which give rise to different boundary value problems.

It is our hope to convince the reader that the physics of the boundary conditions which have to be imposed to model the BET is naturally suggested by the use of the used constrained micromorphic model.

In a second time, we introduce a discrete model for the description of the Bias Extension Test on unbalanced fabrics. To do so, we use long Euler-Bernoulli beams with different bending stiffnesses in the two directions, which are suitably interconnected by rotational and translational springs in such a way that the main characteristics of the experimental Bias Extension Test are described. In particular, we are able to recover in a realistic way both the macroscopic asymmetric shape of the specimen as well as the pattern of the yarns at the mesoscopic scale which include shear strain, bending and slipping. Since the yarns constituting the specimen never experience compression during the BET, we can sensibly affirm that the introduced model of interconnected Euler-Bernouilli beams actually describe, at least qualitatively, the overall behavior of the reinforcement.

Even though the proposed discrete model only involve elastic elements (beams and springs), it is able to catch in a quite realistic way the main features of the deformation of unbalanced fabrics. A point that could be improved in this sense is to introduce some dispersion in the model (friction), following e.g. the methods presented in [35, 57], in order to account for the phenomenon which is experimentally observed and which suggests that, after unloading, the specimen does not perfectly return to its initial undeformed shape.

The results obtained via the discrete model allow us to comfort those obtained via the constrained micromorphic continuum model and they additionally allow to bring more light on the mechanisms of slipping that occur during the BET on unbalanced fabrics.

The paper is organized as follows

- In section 1 we set-up the equilibrium problem for both Cauchy and micromorphic continua. To do so, we introduce suitable spaces of configurations and of admissible variations whose structure is directly related to the kinematical boundary conditions that are imposed in the considered problem. We hence formulate the equilibrium problem for the considered (Cauchy and Micromorphic) continua by means of the use of the Principle of Virtual Work. Finally, we treat in more detail the problem of the equilibrium

of a first gradient continuum by obtaining the irreducible form of the work of internal actions for such a continuum. This irreducible form allows to individuate the type of boundary contact actions which can be introduced in Cauchy media, namely "forces" per unit area. Finally, we explicitly show a method to calculate external contact actions by means of the use of the Principle of Virtual Work: such method is based on a wise choice of particular test functions that allow to isolate forces and double forces on some specific parts of the boundary.

- In section 2 we study the equilibrium of an unbalanced 2D fabric subjected to a Bias Extension Test. This study is carried out following three subsequent steps. First of all the physical problem (BET on unbalanced fabric) is precisely described with particular attention to the description of the imposed kinematical and boundary conditions (see e.g. [10, 13, 35, 47]). Secondly, a discussion concerning the most appropriate continuum model which is needed to describe the physical phenomenon of interest is carried out. We propose a constrained micromorphic model to accomplish this task (see also [31]). Such model is able to account for i) the angle variation between warp and weft yarns, ii) the unbalanced bending stiffness of the two families of fibers and iii) the relative slipping of the yarns by means of the introduction of "equivalent elongations". Last but not least the introduced constrained micromorphic model is seen to be able to introduce in a natural way the boundary conditions which are peculiar of the BET. Finally, we present the numerical simulations of the proposed constrained micromorphic continuum model to show that it is able to satisfactorily describe the experimental evidences.

- In section 3 we introduce the discrete model for the description of the BET by means of the use of Euler-Bernoulli beams suitably interconnected by rotational and translational elastic springs. We show that the obtained results fit well the available experimental evidences both for what concerns the macroscopic and microscopic deformation patterns. In particular, the phenomenon of relative slipping of the yarns is unveiled in a rather precise way so allowing a wise interpretation of the equivalent elongations introduced in the continuum micromorphic model.

We explicitly remark that section 1 contains an introductory theoretical treatise which is convenient to frame the considered mechanical problem in the framework of the Principle of Virtual Work. We believe that such a discussion is indeed very useful for those readers who want to make a clear connection between a neat mathematical formulation of the Principle of Virtual Work and the description of the mechanical phenomena that such principle can provide. Actually, an intelligible and self-consistent disquisition ranging from the mathematical setting to the mechanical interpretation of the Principle of Virtual Work is difficult to be found in academic articles, so that we believe that section 1 represents an added value for the present paper. Some of the introduced notations are voluntarily lightened with respect to those presented in classical more mathematical books (see e.g. [51]) in order to make easier the connection between the mathematical and the mechanical aspects of the same problem. The reader who is not interested in establishing such connection can skip this opening section, directly passing to the mechanical setting-up of the considered problem. On the other hand, the reader who is interested in a more precise and general mathematical formulation of the problem can refer e.g. to [51].

1 The Principle of Virtual Work and the equilibrium of Cauchy and micromorphic continua

In what follows we will call *Cauchy continuum body* a set of material particles occupying the volume B in its reference configuration and whose motion is described by means of a suitably regular, kinematical field $u : B \to \mathbb{R}^3$ which we call the *displacement field* of the considered body. We denote by[1] $\delta u : B \to T\mathbb{R}^3$ the *virtual displacement field* associated to the considered body. Finally, we will denote by ∂B the boundary of B.

Generalizing this definition of Cauchy continuum, we will introduce a simple *micromorphic continuum body* by complementing the previously defined Cauchy continuum with a supplementary, suitably regular, scalar kinematical field $\varphi : B \to \mathbb{R}$, that we generally call *micro-motion*. We denote by[2] $\delta\varphi : B \to T\mathbb{R}$ the virtual variations of the kinematical field φ. We remark that, in the spirit of Mindlin [54] and Eringen [30],

[1]Here and in the sequel we denote by $T\mathbb{R}^3$ the tangent bundle to the manifold $\mathbb{R}^3$. We recall that the virtual variation δu of a displacement field u has the structure $\delta u(X) = (u(X), \delta w(X))$, where $\delta w(X)$ is a vector attached to the Eulerian point $u(X)$.

[2]Here and in the sequel we denote by $T\mathbb{R}$ the tangent bundle to the manifold $\mathbb{R}$. We recall that the virtual variation $\delta\varphi$ of a micro-strain field φ has the structure $\delta\varphi(X) = (\varphi(X), \delta\psi(X))$, where $\delta\psi(X)$ is a vector attached to the image point $\varphi(X)$.

such supplementary kinematical field represents the motion of a microstructure which is embedded in the considered body. Such micro-motion is, in principle, completely independent of the macroscopic motion of the matrix. Nevertheless, in some cases of physical interest, as the one which will be analyzed in this paper, it is worth to relate such micro-descriptors to the derivatives of the macroscopic displacement field. As we will show later on in much more detail, this can be done by constraining the introduced micromorphic model with suitable Lagrange multipliers to be added in the strain energy density, or equivalently, by introducing a penalty term in the energy itself. We want to stress the fact that we prefer to keep a more general micromorphic model and to subsequently constrain its strain energy density in order to let it tend to a second gradient one. This choice is preferable if one wants to interpret in a unique way the external actions of the considered continuum. In fact, (see e.g. [50, 54, 55]) if one starts directly from a second gradient energy, the interpretation of boundary contact actions, namely forces and double-forces, depends on the type of manipulation which is done on the work of internal actions by means of procedures of integration by parts. More particularly, if one decides to stop at a given level of integration by parts, or to continue further to the subsequent level, the definition of force and double force is not the same[3]. When considering micromorphic continua in which only first gradient of the introduced kinematical fields appear in the strain energy density, only one level of integration by parts is possible and then the boundary contact actions are uniquely defined and take immediate physical meaning when framed in the considered physical problem.

The equilibrium of a Cauchy continuum body subjected to given boundary conditions can be studied by means of the Principle of Virtual Work. Such fundamental principle of Mechanics states that a body, subjected to specific external actions, is in equilibrium if the work of internal actions is balanced by the work of external actions. In formulas, we say that a displacement field u^* is an equilibrium configuration if [4]

$$\mathcal{P}^{int}\left(u^*, \delta u\right) + \mathcal{P}^{ext}\left(u^*, \delta u\right) = 0, \tag{1}$$

for any compatible δu. In most cases, the external and internal works can be seen as the first variation of suitable functionals $\mathcal{A}^{int}\left(u\right) : Q \to \mathbb{R}$ and $\mathcal{A}^{ext}\left(u\right) : Q \to \mathbb{R}$, so that the Principle of Virtual Work (1) actually implies the minimization of a functional $\mathcal{A} := \mathcal{A}^{int} + \mathcal{A}^{ext}$. More specifically, we can write

$$\mathcal{P}^{int}\left(u, \delta u\right) + \mathcal{P}^{ext}\left(u, \delta u\right) = \delta\mathcal{A}(u, \delta u) := \lim_{t \to 0^+} \frac{\mathcal{A}\left(u + t\,\delta u\right) - \mathcal{A}(u)}{t}, \tag{2}$$

where we denoted by $\delta\mathcal{A}$ the first variation of the functional $\mathcal{A}$, where $u \in Q$, $\delta u \in T_u$ and the sets Q and T_u will be defined in more detail later on.

Suitably generalizing the definitions given above for first gradient continua, the Principle of Virtual Work can be reformulated for the introduced micromorphic continuum by saying that a couple (u^*, φ^*) is of equilibrium if

$$\mathcal{P}^{int}\left(u^*, \varphi^*, \delta u, \delta\varphi\right) + \mathcal{P}^{ext}\left(u^*, \varphi^*, \delta u, \delta\varphi\right) = 0, \tag{3}$$

for any compatible $(\delta u, \delta\varphi)$.

Again, the external and internal works can be seen as the first variation of suitable functionals $\mathcal{A}^{int}\left(u, \varphi\right) : Q \times D \to \mathbb{R}$ and $\mathcal{A}^{ext}\left(u, \varphi\right) : Q \times D \to \mathbb{R}$, so that the Principle of Virtual Work (3) actually implies the minimization of a functional $\mathcal{A} := \mathcal{A}^{int} + \mathcal{A}^{ext}$. More specifically, we can write

$$\mathcal{P}^{int}\left(u, \varphi, \delta u, \delta\varphi\right) + \mathcal{P}^{ext}\left(u, \varphi, \delta u, \delta\varphi\right) = \delta\mathcal{A}(u, \varphi, \delta u, \delta\varphi) := \lim_{t \to 0^+} \frac{\mathcal{A}\left(u + t\,\delta u, \varphi + t\,\delta\varphi\right) - \mathcal{A}(u, \varphi)}{t}, \tag{4}$$

where we denoted again by $\delta\mathcal{A}$ the first variation of the functional $\mathcal{A}$, where $(u, \varphi) \in Q \times D$, $(\delta u, \delta\varphi) \in T_u \times T_\varphi$ and the sets Q, D, T_u and T_φ will be defined in more detail later on.

Suitable generalizations of the Principle of Virtual Work can be introduced in order to account for inertial and dissipative effects, but, since we deal in this paper only with static problems, we refrain here to present such more complex framework.

The most fundamental questions which have to be confronted to properly set up a mechanical theory by means of the Principle of Virtual Work is to establish:

[3] We need to mention the fact that no common agreement is currently available concerning the choice of different but equally legitimate sets of boundary conditions deriving to different levels of integration by parts. Nevertheless, this is what is found e.g. in [50, 54, 55] and we tend to adopt this viewpoint in the recent times.

[4] We remark that, depending on the conventions which are used for the signs in the definition of the work of internal and external actions, slightly different versions of the Principle of Virtual Work can be found in the literature.

- the constitutive form of the *work of internal actions* in terms of the displacement and, eventually, of the micro-descriptor (such constitutive choice is related to the intrinsic nature of the medium that one wants to study),
- the expression of the *work of external actions*, which allows to establish how the external world acts on the considered medium and to define the concept of force, double force, or other more complex interactions.

As a matter of fact, we can imagine to act on the boundary of the considered body by imposing either

- kinematical (or essential or geometric) boundary conditions: the displacement and/or eventually the micro-descriptor are assigned on some portion Σ_K of the boundary ∂B,
- traction (or natural) boundary conditions: forces and/or, eventually, other more complex external interactions are assigned on some portion Σ_T of the boundary ∂B.

In order to be more general, we can introduce

- The surface Σ_{K_1} on which displacement is assigned and the surface Σ_{K_2} on which we can eventually assign the micro-descriptor φ. Clearly, $\Sigma_K = \Sigma_{K_1} \bigcup \Sigma_{K_2}$, and the two sets Σ_{K_1} and Σ_{K_2} may eventually partially or totally overlap depending on the considered physical problem.
- The surfaces Σ_{T_1} on which we assign forces and Σ_{T_2} on which we can assign more complex interactions and that can as well partially or totally overlap depending on the physical problem in study. We also have $\Sigma_T = \Sigma_{T_1} \bigcup \Sigma_{T_2}$.

If, in the considered physical problems (this may eventually arrive in micromorphic theories), mixed kinematical-traction boundary conditions are applied, also the sets Σ_{K_1} and Σ_{T_2} and/or Σ_{K_2} and Σ_{T_1} may eventually have non-vanishing intersection.

We also explicitly mention that, in order to be able to recover all the possible external interactions, each of the introduced sets Σ_{K_1}, Σ_{K_2}, Σ_{T_1} and Σ_{T_2} may collapse in the empty set or can cover the whole boundary ∂B. Finally, we remark that, by definition, we set $\Sigma_K \bigcup \Sigma_T = \partial B$. Finally, we also mention that we will neglect external volume forces in the following treatment.

1.1 Space of configurations and spaces of admissible variations

Depending on the intrinsic nature of the considered body (first gradient or micromorphic), the expressions for the work of internal and external actions take specific forms which will be better specified later on.

Independently of the specific form taken by the internal and external work, we want to underline here that the problem of finding the equilibrium configuration of a given continuum (Cauchy or micromorphic) subjected to specific boundary conditions reduces to the problem of finding, in suitable sets, the kinematical fields which satisfy the Principle of Virtual Work ((1) or (3)) for any virtual admissible variations.

We start by introducing the equilibrium problem for a Cauchy continuum, defining a suitable set Q, called *space of configurations* of the considered medium which contains information about the kinematical constraints which must be verified by the displacement field. More precisely, we define the space of configurations for a Cauchy continuum as[5]

$$Q = \{u \ \mid \ u = \bar{u} \ \text{ on } \ \Sigma_{K_1}\}, \tag{5}$$

where $\bar{u}$ is a suitably assigned function. Roughly speaking, the set Q represents the set in which we look for the solution of our minimization problem and contains only those displacement fields which satisfy the imposed kinematical boundary conditions.

On the other hand, we define the set of admissible variations as

$$T_u = \{\delta u \ \mid u + \delta u \in Q\}. \tag{6}$$

[5]We remark that the set Q should also contain informations concerning the desired regularity on u, but we limit ourselves here to talk about "suitably regular" functions.

We explicitly remark that, being $u = \bar{u}$ on Σ_{K_1}, in order to have δu belonging to the set of admissible variations, one must have that $\bar{u} + \delta u = \bar{u}$ on Σ_{K_1}. This clearly implies that $\delta u = 0$ on Σ_{K_1}, and hence the set of admissible variations takes the form $T_u = \{\delta u \ \mid \delta u = 0 \ \text{ on } \ \Sigma_{K_1}\}$.With the introduced notations, we can formulate the equilibrium problem for a Cauchy continuum as:

Find $u^* \in Q$ *such that* $\mathcal{P}^{int}(u^*, \delta u) + \mathcal{P}^{ext}(u^*, \delta u) = 0 \quad$ *for any* $\delta u \in T_{u^*}$.

The setting-up of the equilibrium problem for a micromorphic continuum can be obtained, suitably generalizing what done for Cauchy continua. In particular, a supplementary set D must be defined to specify the space of configurations for such continuum[6]:

$$D = \{\varphi \mid \ \varphi = \bar{\varphi} \ \text{ on } \ \Sigma_{K_2}\},$$

where $\bar{\varphi}$ is a suitably assigned function. Roughly speaking, the set D represents the set in which we look for the solution for the micro-motion of our minimization problem and contains only those micro-motions which satisfy the imposed kinematical boundary conditions.

Moreover, we define a supplementary set of admissible variations as

$$T_\varphi = \{\delta\varphi \ \mid \varphi + \delta\varphi \in D\}.$$

With the introduced notations, we can formulate the equilibrium problem for a micromorphic continuum as:

Find $(u^*, \varphi^*) \in Q \times D$ *such that* $\mathcal{P}^{int}(u^*, \varphi^*, \delta u, \delta\varphi) + \mathcal{P}^{ext}(u^*, \varphi^*, \delta u, \delta\varphi) = 0 \quad$ *for any* $(\delta u, \delta\varphi) \in T_{u^*} \times T_{\varphi^*}$.

1.2 The example of the equilibrium of a first gradient continuum

As it has been previously pointed out, in order to establish the equilibrium problem for a given continuum body subjected to specific external interactions, the expressions of both the work of internal and external actions must be specified.

For a first gradient continuum the work of internal actions is defined through the definition of the action functional $\mathcal{A}^{int}$ which can be introduced in the static case as[7]

$$\mathcal{A}^{int} = -\int_B W(\nabla u)\, dv,$$

where W is the strain energy density which, in a first gradient model, constitutively depend only on the first gradient of displacement.

In the case of first gradient theories we can hence recognize that the work of internal actions can be written as [8]

$$\begin{aligned} \mathcal{P}^{int}(u, \delta u) &= -\int_B \delta W(\nabla u)\, dv = -\int_B \left\langle \frac{\partial W}{\partial \nabla u} \ , \ \nabla \delta u \right\rangle dv \\ &= \int_B \left\langle \mathrm{Div}\left(\frac{\partial W}{\partial \nabla u}\right) \ , \ \delta u \right\rangle dv - \int_{\partial B} \left\langle \frac{\partial W}{\partial \nabla u} \cdot n \ , \ \delta u \right\rangle ds, \end{aligned} \tag{7}$$

where to obtain the last identity the divergence theorem has been used. Equation (7) furnishes the *irreducible expression of the work of internal actions* for a first gradient continuum. This means that no more integrations by parts can be performed to ulteriorly manipulate this expression of $\mathcal{P}^{int}$. It can be remarked from such irreducible form of the internal work that, as far as the boundary ∂B is concerned, only quantities expending work on the virtual displacement δu (i.e. forces) can be recognized. It is for this reason that, based on the validity of the Principle of Virtual Work, we can affirm that the only boundary external actions that can be sustained by a first gradient continuum are forces per unit area, i.e. external actions expending work on

[6] We remark that the set D should also contain informations concerning the desired regularity on φ, but we limit ourselves here to talk about "suitably regular" functions.

[7] Classically, in the dynamic case the internal action functional is defined as the space-time integral of the Lagrangian density $\mathcal{L} = T - W$, where T is the kinetic energy density. In the particular case of statics, the minus sign remains after the due simplifications.

[8] The operator Div stands for the classical divergence operator. Being A a tensor field of any order $n > 0$, we define its divergence as the $n-1$ tensor $(\mathrm{Div}A)_{i_1,\dots i_{n-1}} = A_{i_1,\dots i_n, i_n}$. Finally $\langle a, b\rangle = a_{i_1,\dots i_n}\, b_{i_1,\dots i_n}$ indicates the scalar product between two tensors of any order $n \geq 1$ and the Einstein convention of sum over repeated indices is used.

δu. These observations are at the origin of the introduction of the work of external actions for first gradient continua in the form[9]

$$\mathcal{P}^{ext}(u, \delta u) = \int_{\Sigma_{T_1}} \langle f, \delta u \rangle \, ds, \tag{8}$$

where $f : B \to \mathbb{R}^3$ is a suitable function assigned on Σ_{T_1}.

Once assigned the specific form for the work of internal and external actions, the equilibrium problem for a first gradient continuum can be hence reformulated as follows:

Find $u^* \in Q$ *such that* $\mathcal{P}^{int}(u^*, \delta u) + \mathcal{P}^{ext}(u^*, \delta u) = 0 \quad$ *for any* $\delta u \in T_{u^*}$,

where now $\mathcal{P}^{int}$, $\mathcal{P}^{ext}$, Q and T_{u^*} are given by (7), (8), (5) and (6) respectively.

1.2.1 Evaluation of the reaction force corresponding to an imposed boundary displacement.

Once that the solution u^* of the equilibrium problem for a first gradient continuum has been found following the steps presented in subsection 1.2, it may be interesting to know which is the reaction force acting on Σ_{K_1} that balances the displacement $\bar{u}$ which has been imposed on the surface Σ_{K_1} itself. In other words, we are looking for the force that one should apply on the portion of the boundary Σ_{K_1} in order to produce the displacement $\bar{u}$ on Σ_{K_1} and the displacement field u^* within the considered body. In order to answer to this question, it is possible to pass again through the Principle of Virtual Work, but imagining now that a work of external forces must be introduced also on the portion of the boundary Σ_{K_1}. We hence re-define the external work (8) by adding an additional term as follows

$$\mathcal{P}^{ext}(u, \delta u) = \int_{\Sigma_{T_1}} \langle f, \delta u \rangle \, ds + \int_{\Sigma_{K_1}} \langle f_R, \delta u \rangle \, ds. \tag{9}$$

The reaction force can hence be calculated by writing the Principle of Virtual Work as

$$\int_B \left\langle \mathrm{Div}\left(\frac{\partial W}{\partial \nabla u^*}\right) \, , \, \delta u \right\rangle dv - \int_{\partial B = \Sigma_{T_1} \bigcup \Sigma_{K_1}} \left\langle \frac{\partial W}{\partial \nabla u^*} \cdot n \, , \, \delta u \right\rangle ds + \int_{\Sigma_{T_1}} \langle f, \delta u \rangle \, ds + \int_{\Sigma_{K_1}} \langle f_R, \delta u \rangle \, ds = 0 \tag{10}$$

and imposing that it must be valid for any arbitrary displacement δu. Such identity must be satisfied, in particular, for a virtual displacement field $\delta \bar{u}$ which is such that

- $\delta \bar{u}$ is constant on Σ_{K_1}
- $\delta \bar{u}$ is continuous on ∂B
- $\delta \bar{u}$ is vanishing outside Σ_{K_1} except on a suitably small region in order to preserve continuity with the imposed displacement at the boundary.

For such particular test function, the Principle of Virtual Work (10) implies

$$\int_{\Sigma_{K_1}} \langle f_R, \delta \bar{u} \rangle \, ds = \left\langle \int_{\Sigma_{K_1}} f_R \, ds \, , \delta \bar{u} \right\rangle = \left\langle \int_{\Sigma_{K_1}} \frac{\partial W}{\partial \nabla u^*} \cdot n \, ds \, , \, \delta \bar{u} \right\rangle.$$

The constant test field $\delta \bar{u}$ can hence be simplified on the two sides and, introducing the quantity $R := \int_{\Sigma_K} f_R \, ds$, we can finally write

$$R = \int_{\Sigma_{K_1}} \frac{\partial W}{\partial \nabla u^*} \cdot n \, ds. \tag{11}$$

We call R the *reaction force* associated to the imposed displacement $\bar{u}$ on Σ_{K_1}. We will see that the fact of computing the reaction forces on the basis of the procedure shown here may be of interest for comparing the results of the performed numerical simulations to the experimental data. In fact, when a standard testing machine measures a "force" associated to an imposed displacement, it is actually measuring a resultant force on the considered boundary.

We explicitly remark that, an equivalent way to calculate the reaction force can be found considering the work of internal forces before integrating by parts as given in the first equality in expression (7), i.e.

$$\mathcal{P}^{int}(u, \delta u) = -\int_B \left\langle \frac{\partial W}{\partial \nabla u} \, , \, \nabla \delta u \right\rangle dv.$$

[9] We recall once again that, to the sake of conciseness, we suppose in this paper that bulk external actions are vanishing.

With reasoning analogous to the previous ones, if we write the Principle of Virtual Work evaluated in the equilibrium solution u^*, we have

$$-\int_B \left\langle \frac{\partial W}{\partial \nabla u^*} \ , \ \nabla \delta u \right\rangle dv + \int_{\Sigma_{T_1}} \langle f, \delta u \rangle \, ds + \int_{\Sigma_{K_1}} \langle f_R, \delta u \rangle \, ds = 0,$$

which must be satisfied for any δu. If we hence choose a particular test function $\delta \bar{u}$ such that

1. $\delta \bar{u}$ is constant on Σ_{K_1}
2. $\delta \bar{u}$ is continuous on ∂B
3. $\delta \bar{u}$ is an arbitrarily assigned, non-vanishing function outside Σ_{K_1}

we can evaluate the reaction force by noticing that

$$\langle R, \delta \bar{u} \rangle = \int_B \left\langle \frac{\partial W}{\partial \nabla u^*} \ , \ \nabla \delta \bar{u} \right\rangle dv - \int_{\Sigma_{T_1}} \langle f, \delta \bar{u} \rangle \, ds. \tag{12}$$

We explicitly remark that Eq. (12) is a scalar equation, which means that the three components of the vector R cannot be directly calculated only using such equation. Nevertheless, if we choose suitable test functions $\delta \bar{u}$ which are aligned with one of the directions of the used reference system, we can arrive to evaluate separately the components of R. In particular, let $\{e_i\}_{i \in \{1,2,3\}}$, be an orthonormal basis with respect to which we want to evaluate the three components $R_i = \langle R, e_i \rangle$ of the reaction force R. We choose a test function $\delta \bar{u}$ which possesses all the characteristics previously listed except that the point 1. is replaced by

- $\delta \bar{u}$ is equal to e_i on Σ_{K_1}.

In this case the component R_i can be easily calculated according to Eq. (12).

Clearly, if the problem is well formulated, the value of the reaction R calculated with expression (11) must coincide with the one calculated using expression (12). The second way of evaluating the reaction force has many advantages, especially when we want to do it numerically. Indeed, it is always more stable to numerically evaluate a volume integral than a surface integral. It is for this reason that, for the case of micromorphic continua shown in the next section, we will limit ourselves to show how to calculate reaction forces and double-forces, by passing trough the evaluation of volume integrals.

2 Equilibrium of a 2D unbalanced woven fabric modeled as an orthotropic micromorphic continuum

It has been known since the pioneering works by Piola [70], Cosserat [14], Mindlin [54], Toupin [86], Eringen [30], Green and Rivlin [38] and germain1973method [36] that many microstructure-related effects in mechanical systems can be still modeled by means of continuum theories. It is known since then that, when needed, the placement function must be complemented by additional kinematic descriptors, called sometimes micro-structural fields. More recently, these generalized continuum theories have been widely developed (see e.g. [25, 23, 24, 22, 1, 33, 87, 32, 34, 29, 28]) to describe the mechanical behavior of many complex systems, such as e.g. porous media [19, 48, 80, 81], capillary fluids [11, 16, 18, 21, 17], exotic media obtained by homogenization of heterogeneous media [3, 69, 82]. Interesting applications on wave propagation in such generalized media has also gained attention in the recent years for the possible application of this kind of materials to passive control of vibrations and stealth technology (see e.g. [20, 49, 71, 78]).

In this section, we will frame the problem of determining the equilibrium of a 2D, unbalanced, woven reinforcement modeled as a micromorphic material, in the spirit of section 1. With this precise aim in mind, we will first present the particular physical problem that we want to study, then we will propose suitable expressions for the work of internal and external actions and we will introduce the adapted spaces of configurations and of admissible variations. We will finally formulate the equilibrium problem for the introduced micromorphic continuum and we will solve it by means of suitable numerical simulations.

2.1 The physical problem: bias extension test on an unbalanced fabric

We consider in this subsection the description of the physical problem that we want to analyze and for which we will develop a suitable mechanical second constrained micromorphic model in the next subsection. The material that we consider here is an unbalanced fabric, i.e. a fibrous reinforcement in which the warp and weft yarns have very different thickness due to the fact that they are constituted by a significantly different number of fibers. This unbalance is reflected in a different mechanical behavior of the two orders of yarns. In order to sketch a simplified description of the mechanical behavior of unbalanced fabrics we can notice that

- the yarns can be supposed to be *quasi-inextensible* in both the warp and weft directions, due to the very high tensile resistance of the constituent carbon fibers. This means that, notwithstanding the different thickness of the yarns, we can suppose that they do not sensibly elongate. Actually, an initial apparent elongation of the yarns due to *decrimping* can be eventually observed when testing the woven material, but it is reasonable to suppose that such apparent elongation, if present, has eventually the same characteristics in both directions.
- The warp and weft being strongly unbalanced, we can infer that they possess very *different bending stiffnesses*. More particularly, the thick yarns are sensible to exhibit a higher resistance to bending than the thin ones.
- Depending on the nature of the externally applied load and/or boundary conditions, the yarns can experience some *relative slipping*. More precisely, it is possible that the contact point between two yarns can move during the deformation of the macroscopic piece.

We are interested in this paper to the description of a Bias Extension Test on an unbalanced fabric of the type described above. More precisely, the specimens object of the study are rectangular carbon fiber interlocks (the height must at least 2.5 times longer than the basis) with unbalanced yarns oriented at $\pm 45°$ with respect to the long side of the specimen (see Fig. 2). The two shorter edges of the specimens are clamped in suitable devices which assure the following kinematical boundary conditions

- vanishing displacement on Σ_1,
- constant assigned displacement u_0 on Σ_2,
- angle between warp and weft blocked at $45°$ on Σ_1 and Σ_2 (i.e. vanishing angle variation between the two families of yarns during the motion of the fabric).

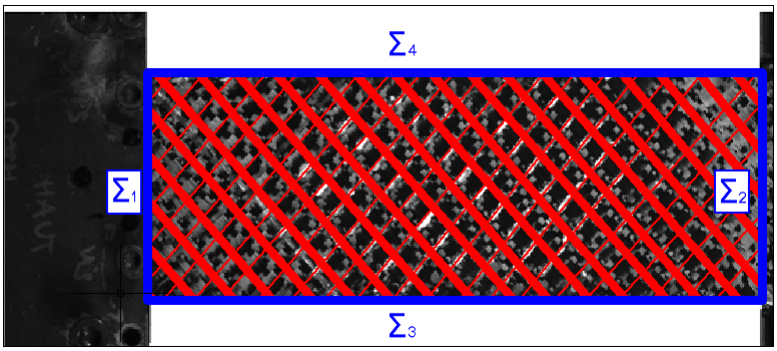

Figure 2: Experimental set-up for a bias extension test on an unbalanced fabric: it must be $|\Sigma_4| \geq 2.5\,|\Sigma_1|$. For the considered experimental test we have $|\Sigma_1| = 70\,mm$ and $|\Sigma_4| = 220\,mm$. Moreover, the specimen is $15mm$ thick, but we suppose that this has no influence on the results, i.e. no displacement neither deformation occur out of the plane of the fabric.

The experimental result of the performed mechanical test is a S-shaped macroscopic deformation as the one presented in figure 3.

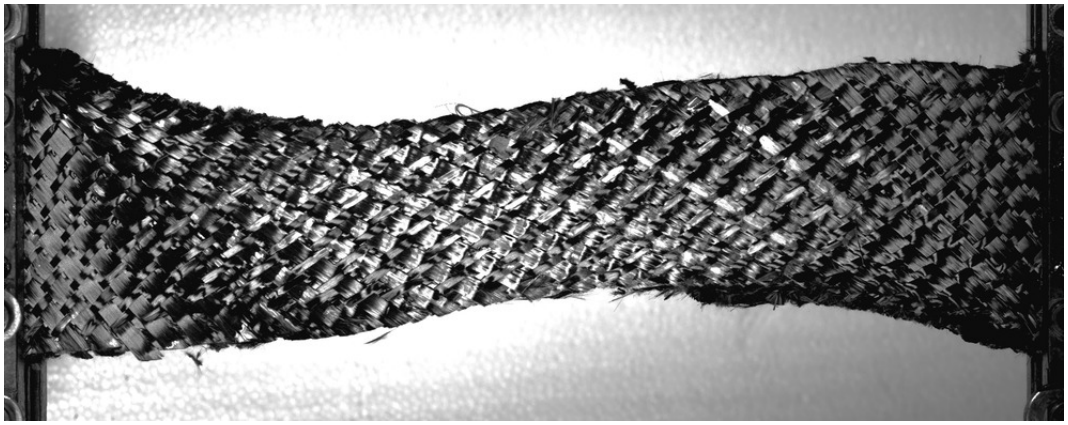

Figure 3: Experimental deformed shape for an imposed displacement $u_0 = 56\,mm$.

The obtained asymmetric shape is related to the fact that the material properties and, in particular, the bending stiffnesses of the yarns are not the same in the two privileged material directions. Moreover, due to the applied boundary conditions, some non-negligible slipping of the yarns is also observed, above all for what concerns the central part of the specimen in which yarns with two free ends are located.

We will more precisely describe later which is the precise pattern of the yarns inside the considered specimen. On the other hand, we want to point out here that, indeed, a sensible *differential bending* can be observed in the considered specimen. In fact, the thin yarns are seen to be sensibly bent in some thin transition layers, while the thick yarns do not bend at all as highlighted in Fig. 4.

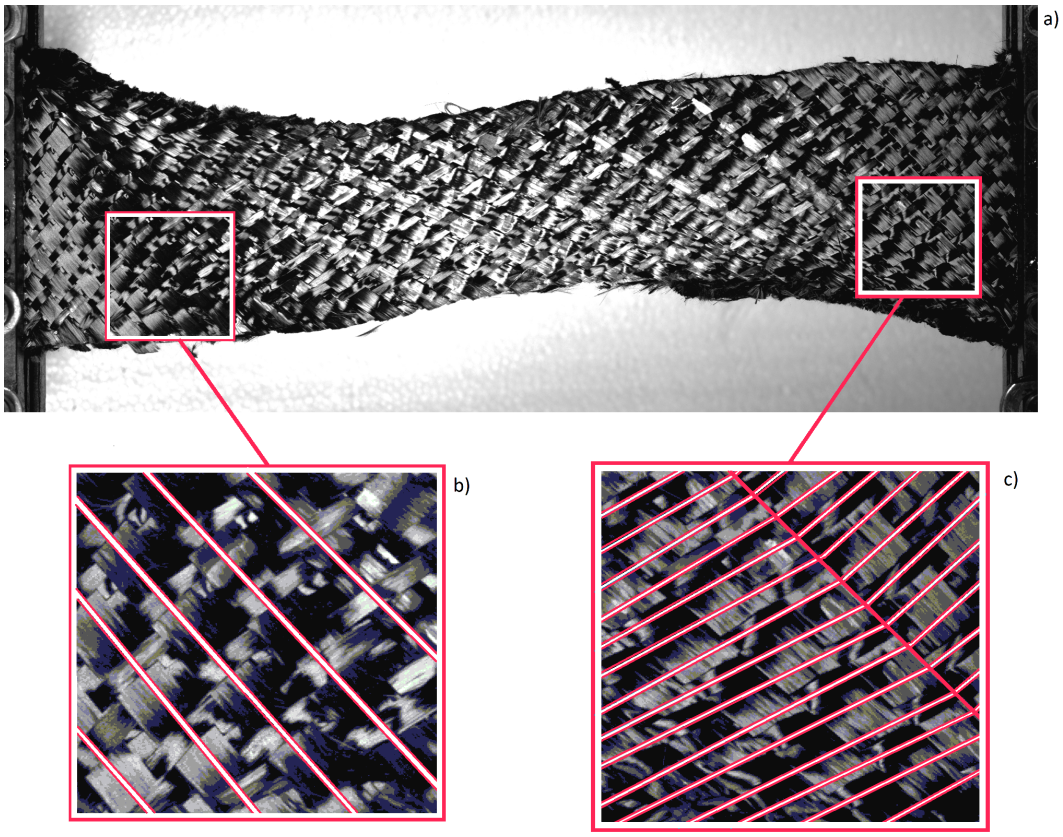

Figure 4: Differential bending of the thick (b) and thin (c) yarns as observed in the experimental deformed shape (a).

Such differential bending is certainly at the origin of the asymmetric deformed shape.

2.2 The equilibrium problem for an orthotropic micromorphic continuum subjected to Bias Extension Test

In this subsection we want to set up a consistent continuum mechanical framework which is able to account for

- the presence of *two preferred material directions* inside the macroscopic body,
- the unbalance of the fabric which, for what said in subsection 2.1, basically means that the two families of yarns have *different bending stiffnesses*,
- the *relative slipping* of the yarns.

In order to do so, we need to remark that the desired continuum model (constrained micromorphic) must be such that

- the chosen first gradient constitutive laws account for the *orthotropy* of the considered medium,
- it allows to describe the *curvature* of material lines. Moreover, the resistance to curvature must be different for the two family of yarns, which means that the introduced constitutive laws must account for different bending stiffnesses for the two families of yarns. In order to reduce the adopted micromorphic model to a second gradient one, suitable constrains must be introduced in order to let higher order derivatives appear in the strain energy density,
- notwithstanding the quasi-inextensibility of the carbon yarns, it includes equivalent elongation modes in the yarns directions in order to indirectly account for the slipping of the fibers. The fact of considering such elongation modes, also allows the model the possibility of describing the initial decrimping of the yarns.

In order to formulate the equilibrium problem for the considered continuum subjected to a Bias Extension Test in the general framework introduced in section 1, we need to specify the particular form that $\mathcal{P}^{int}$, $\mathcal{P}^{ext}$, Q , D, T_u and T_φ take in the treated example.

2.2.1 Work of internal actions for a 2D, orthotropic, constrained micromorphic continuum

We start by specifying the expression of the work of internal actions which is suitable to describe the deformation of the considered system. To do so, we start by recalling classical results for first gradient, hyperelastic orthotropic continua which prescribe the functional dependence that the strain energy density of an orthotropic continuum must have on the Cauchy-Green strain tensor $C = F^T \cdot F$ (see e.g. [8, 7, 13, 41, 45, 43, 65, 66, 72, **?**, 84]).

Here and in the sequel, we denote by $\chi : B \to \mathbb{R}^3$ the placement function associated to the considered body that associates to any material particle $X \in B$ its current position x in the deformed configuration and which can be related to the displacement field by means of the relation $\chi = u + X$. Moreover, we denote by $F = \nabla\chi$ the space gradient of the introduced placement field.

We start by assuming that the strain energy density can be given in the form

$$W(C, \nabla\varphi) = W_I(C) + W_{II}(\nabla\varphi). \tag{13}$$

Representation theorems for 3D orthotropic first gradient materials are available in the literature (see e.g. [72, 44, 15]), which state that the functional dependence of the strain energy density on the strain tensor C must be given in terms of its invariants $i_O := \{i_1, i_4, i_6, i_8, i_9, i_{10}\}$, where the introduced invariants are defined in table 1 in which also their physical interpretation can be found.

Explicit expressions for the strain energy potential as function of the invariants i_O which are suitable to describe the real behavior of orthotropic hyperelastic materials are difficult to be found in the literature. Certain constitutive models are for instance presented in [45], where some polyconvex energies for orthotropic materials are proposed to describe the deformation of rubbers in uniaxial tests. Explicit anisotropic hyperelastic potentials for soft biological tissues are also proposed in [42] and reconsidered in [5, 79] in which their polyconvex approximations are derived. Other examples of polyconvex energies for anisotropic solids are given in [85]. It is even more difficult to find in the literature reliable constitutive models for the description

of the real behavior of fibrous composite reinforcements at finite strains but some attempts can be for instance recovered in [2, 13]. Furthermore, the mechanical behavior of composite preforms with rigid organic matrix (see e.g. [27, 53, 52, 67]) is quite different from the behavior of the sole fibrous reinforcements (see e.g. [12]) rendering the mechanical characterization of such materials a major scientific and technological issue.

Invariant	Expression	Meaning in terms of deformation
i_1	$\mathrm{tr}(C)$	Averaged changes of length
i_4	$m_1 \cdot C \cdot m_1$	Local stretch in the direction m_1
i_6	$m_2 \cdot C \cdot m_2$	Local stretch in the direction m_2
i_8	$m_1 \cdot C \cdot m_2$	Angle variation between the directions (m_1, m_2)
i_9	$m_1 \cdot C \cdot m_3$	Angle variation between the directions (m_1, m_3)
i_{10}	$m_2 \cdot C \cdot m_3$	Angle variation between the directions (m_2, m_3)

Table 1: Invariants of the Green-Lagrange strain tensor in the orthotropic case. The vectors m_1 and m_2 are unit vectors in the two privileged directions of the material and $m_3 := m_1 \times m_2$.

For the particular 2D case that we study here we assume that the first gradient energy takes the following particular constitutive form

$$W_I(C) = \frac{1}{2} K_{el} \left[(\sqrt{i_4} - 1)^2 + (\sqrt{i_6} - 1)^2 \right] + \frac{1}{2} K_{sh} i_8^2, \tag{14}$$

where the parameters K_{el} and K_{sh} are assumed to be constant. The constitutive choice (14) can be motivated by noticing that the invariants i_9 and i_{10} represent out-of-plain angle variations of the yarns which are not considered in the present 2D case. Moreover, in a first instance, the isotropic invariant i_1 can be considered to be uninfluential in the considered orthotropic case.

It must be remarked that this simple quadratic choice for the first gradient strain energy density, even if providing geometric non-linearities, could be not sufficiently general to describe larger deformations for which more complex hyperelastic constitutive laws should be introduced. More than that, since for very large strains the integrity of the material starts to be affected due to the excessive slipping, there is no interest in attempting the modeling of the targeted unbalanced materials after a given strain threshold. In order to precisely identify the maximum strain that the material can withstand before failure due to excessive slipping, more experimental campaigns should be carried out. We limit ourselves here to remark that:

- After a first threshold the material behavior starts to present a softening (see experimental pattern in Fig. 8) which can be directly related to slipping. To model such behavior, more general hyperelastic laws with respect to the one presented in this paper should be introduced, but this falls outside the scope of the present work.
- If the experiment is prolonged, the slipping becomes so important that the integrity of the material starts to be affected and some yarns are pulled out of the specimen. In this case, both discrete and continuum model loose their predictability.

In summary, we are saying that, with the considered constitutive choice and when remaining in the moderate strain regime, the main first gradient deformation modes allowed in the deformation of the considered material are

- the angle variation i_8 between the warp and weft direction
- the equivalent elongations i_4 and i_6 in the directions of the warp and weft which account for decrimping and, eventually for slipping.

As for the micromorphic energy, we make the following particular constitutive choice

$$W_{II}(\nabla\varphi) = \frac{1}{2} \langle \alpha, \nabla\varphi \rangle^2 = \frac{1}{2} \left(\alpha_1 \varphi_{,1} + \alpha_2 \varphi_{,2} \right), \tag{15}$$

where the vector $\alpha = (\alpha_1, \alpha_2)$ is the vector of constant micromorphic elastic parameters whose components α_1 and α_2 have to be different to account for the unbalance of the microscopic characteristics of the material.

Moreover, we denoted by $\varphi_{,1}$ and $\varphi_{,2}$ the space derivatives of φ with respect to the space coordinates in the directions m_1 and m_2 (warp and weft) respectively.

We explicitly remark at this point that we want to give a precise physical meaning to the micro-descriptor φ in order to catch at best the experimental behaviors described in subsection 2.1. We have pointed out that a supplementary deformation mode with respect to classical first gradient ones must be introduced in order to catch all the physics of the considered problem. More particularly, additionally to angle variations (i_8) and equivalent elongations in the yarns' directions (i_4 and i_6), we need to account for the bending of the two families of fibers. It is known (see also [26, 31]) that bending strains of the fibers inside the considered macroscopic specimen can be accounted for by introducing second derivatives of the displacement field in the strain energy density. In particular, such bending of the yarns can be related to the space gradient of the angle variation i_8: if sharp variations of angle between warp and weft occur in small regions inside the specimen, it means that the yarns must necessarily bend in order to rapidly change their direction and give rise to such angle variation.

In the light of such remarks, it is sensible to suppose that the introduced micro-descriptor φ must be indeed related to the angle variation i_8: if, for example, we let φ tend to i_8, then expression (15) for the strain energy density accounts for space derivatives of the angle variation and hence, finally, for the bending of the two families of yarns. Indeed, (see also [26, 31]), it may be rather easily inferred how $i_{8,1}$ can be interpreted as the bending of the yarns disposed in the m_1 direction and, analogously, $i_{8,2}$ represents the bending of the yarns aligned in the m_2 direction.

Based on the physics of the problem discussed in the previous subsection, we do not introduce second gradient effects related to the gradients of the other invariants. We are then excluding that sharp spacial changes of elongation occur in the considered material.

At this point, the reader may believe that the fact of considering a micromorphic medium is redundant for treating the considered problem of the Bias Extension Test, since a second gradient model could have been directly introduced, instead of constraining a micromorphic model to become a second gradient one. Nevertheless, the intermediary step of passing through a micromorphic model is essential, at least for two reasons

- the imposed boundary conditions take a precise and unique meaning
- the numerical implementation of the considered problem is more easily treatable since lower order differential equations are involved.

The first point of the unique meaning of the imposed boundary conditions is crucial if one wants to deal with a model which has an easily recognizable physically grounded interpretation. In fact, as far as second gradient theories are concerned, the boundary conditions that can be imposed may take different, but equally legitimate, forms for the same physical problem (see e.g. [50]): for example, in a second gradient theory, a given angle can be imposed either by directly assigning the angle or by suitably choosing the components of the normal derivative of displacement on the boundary. Depending on whether one choice of the kinematical conditions or the other one is made, the dual traction counterparts (dual of the angle variation or of the normal derivative) have different expressions and the definition of the force can be also shown to be non-equivalent in the two cases. Such non-uniqueness of the way of imposing second gradient boundary conditions is directly related to the number of integration by parts which one decides to make in the expression of the internal work: in second gradient theories, the second gradient of the virtual displacement can be integrated by parts twice, by making use of the standard divergence theorem and of the surface divergence theorem.

On the other hand, micromorphic models only involve first gradients of the introduced kinematical fields, so that only one level of integration by parts can be conceived (only the standard divergence theorem is used in a micromorphic model). This fact, avoids any sort of indeterminacy for the imposable boundary conditions when micromorphic models are considered (see e.g. also [6]).

In order to implement the fact that we want to constrain the micromorphic energy (13) to a second gradient one, we need to introduce a suitable Lagrange multiplier Λ with associated strain energy density W_Λ

$$W_\Lambda(\Lambda, i_8, \varphi) = \Lambda\,(\varphi - i_8) \tag{16}$$

In this constrained framework the global energy of the system is not simply (13), but must be complemented with this additional coupling term and in the considered 2D case becomes

$$W(i_4, i_6, i_8, \varphi, \nabla\varphi, \Lambda) = W_I(i_4, i_6, i_8) + W_{II}(\nabla\varphi) + W_\Lambda(\Lambda, i_8, \varphi). \tag{17}$$

We explicitly mention that, the introduction of the Lagrange multiplier Λ does not modify the definition of the set D.

According to the constitutive choices (14) and (16), the work of internal actions of the considered 2D, orthotropic, constrained micromorphic continuum can be written as

$$\mathcal{P}_{II}^{int} = \delta\mathcal{A}^{int} = -\delta\int_B (W_I + W_{II} + W_\Lambda)\, dv = -\int_B (\delta W_I + \delta W_{II} + \delta W_\Lambda)\, dv.$$

Computing the first variation of the introduced internal action functional, we can write

$$\mathcal{P}_{II}^{int} = -\int_B \left[\frac{\partial W_I}{\partial i_4}\delta i_4 + \frac{\partial W_I}{\partial i_6}\delta i_6 + \left(\frac{\partial W_I}{\partial i_8} + \frac{\partial W_\Lambda}{\partial i_8}\right)\delta i_8 + \frac{\partial W_{II}}{\partial \nabla\varphi}\delta\nabla\varphi + \frac{\partial W_\Lambda}{\partial\varphi}\delta\varphi + \frac{\partial W_\Lambda}{\partial\Lambda}\delta\Lambda\right] dv,$$

which for the particular constitutive choice made to treat the physical example considered in this paper, takes the particular form

$$\begin{aligned}\mathcal{P}_{II}^{int} = \int_B \Bigg[&-\frac{1}{2}K_{el}\left(1-\frac{1}{\sqrt{i_4}}\right)\delta i_4 - \frac{1}{2}K_{el}\left(1-\frac{1}{\sqrt{i_6}}\right)\delta i_6 - (K_{sh}i_8 - \Lambda)\,\delta i_8 \\ &- \langle\alpha,\nabla\varphi\rangle\,\langle\alpha,\nabla\delta\varphi\rangle - \Lambda\,\delta\varphi - (\varphi - i_8)\delta\Lambda\Bigg]\, dv.\end{aligned} \tag{18}$$

Considering the definitions of the invariants given in table (1), it can be checked that

$$\delta i_4 = m_1\cdot\delta\left(F^T\cdot F\right)\cdot m_1 = 2\,(F\cdot m_1)\cdot(\delta F\cdot m_1)$$

$$\delta i_6 = m_2\cdot\delta\left(F^T\cdot F\right)\cdot m_2 = 2\,(F\cdot m_2)\cdot(\delta F\cdot m_2)$$

$$\delta i_8 = m_1\cdot\delta\left(F^T\cdot F\right)\cdot m_2 = (F\cdot m_2)\cdot(\delta F\cdot m_1) + (F\cdot m_1)\cdot(\delta F\cdot m_2)\,,$$

so that, replacing such expressions in the first three terms of the internal work (18), recalling that $\delta F = \nabla(\delta\chi) = \nabla(\delta u)$, suitably integrating by parts each term and using the divergence theorem we finally get

$$\begin{aligned}\mathcal{P}_{II}^{int} = &\int_B \left\langle \mathrm{Div}\left[K_{el}\left(1-\frac{1}{\sqrt{i_4}}\right)(F\cdot m_1\otimes m_1)\right] + \mathrm{Div}\left[K_{el}\left(1-\frac{1}{\sqrt{i_6}}\right)(F\cdot m_2\otimes m_2)\right]\,,\,\delta u\right\rangle\, dv \\ &+\int_B \langle\ \mathrm{Div}\left[\ (K_{sh}\,i_8-\Lambda)\ F\cdot(m_1\otimes m_2 + m_2\otimes m_1)\ \right],\ \delta u\ \rangle\ dv - \int_B(\varphi - i_8)\delta\Lambda\, dv \\ &-\int_{\partial B}\left[K_{el}\left(1-\frac{1}{\sqrt{i_4}}\right)(m_1\cdot n) + (K_{sh}\,i_8-\Lambda)\,(m_2\cdot n)\right]\ \langle\ (F\cdot m_1)\ ,\ \delta u\ \rangle\ ds \\ &-\int_{\partial B}\left[K_{el}\left(1-\frac{1}{\sqrt{i_6}}\right)(m_2\cdot n) + (K_{sh}\,i_8-\Lambda)\,(m_1\cdot n)\right]\ \langle\ (F\cdot m_2)\ ,\ \delta u\ \rangle\ ds \\ &+\int_B\ [\alpha\cdot\nabla(\langle\ \alpha,\nabla\varphi\ \rangle) - \Lambda]\ \delta\varphi - \int_{\partial B}\langle\ \alpha,\nabla\varphi\ \rangle\,\langle\ \alpha,n\ \rangle\ \delta\varphi\end{aligned} \tag{19}$$

where we denoted by n the unit normal to the Lagrangian boundary ∂B. We explicitly remark that imposing arbitrary variations $\delta\Lambda$ implies the desired constraint $\varphi = i_8$.

The expression (19) is the *irreducible form of the work of internal actions* for the considered constrained micromorphic medium. We explicitly remark that, the boundary contact actions intervening in the considered

problem expend work on δu (forces) and on $\delta\varphi$ (double-forces). As far as the boundary ∂B is concerned, it can be inferred from Eq. (19) that the dual quantity to the virtual displacement δu contains informations about the first gradient deformations i_4, i_6, i_8 as well as the Lagrange multiplier Λ. We are in some way saying that the internal force which would eventually balance an externally applied force involve deformation mechanisms related to elongations of the warp and weft, angle variations, but also (through the Lagrange multiplier Λ) some microstructure-related deformation modes. On the other hand, the internal double-force (couple) which would eventually balance an externally applied double force, involve deformation mechanisms associated to the local bending of the yarns (first derivatives of the angle variation $\varphi = i_8$).

Analogously to what done in subsection 1.2.1, we could use this irreducible expression of the work of internal forces to suitably calculate the reaction forces and double-forces on the part of the boundary where we assign the kinematical constraints. Nevertheless, since in our numerical simulations we only use the second method to calculate such reactions (passing through the evaluation of volume integrals), we will limit ourselves to present it in subsection 2.2.4.

2.2.2 Work of external actions for the considered constrained micromorphic continuum

According to the procedure shown in the previous section, in order to formulate the equilibrium problem for a given continuum, the work of external actions must be given on the portion of the boundary $\Sigma_T = \Sigma_{T_1} \bigcup \Sigma_{T_2}$ where tractions are assigned. According to the irreducible expression (19) which we consider for the work of internal actions, the external work that balances the boundary terms of the internal one, must contain "*forces*" f that expend work on the virtual displacement δu and "*double-forces*" τ that expend work on the virtual angle variation $\delta\varphi$. In particular, the work of external forces for the considered micromorphic continuum is assumed to take the form

$$\mathcal{P}_{II}^{ext} = \int_{\Sigma_{T_1}} \langle f, \delta u \rangle \, ds + \int_{\Sigma_{T_2}} \tau \, \delta\varphi \, ds. \tag{20}$$

For the particular case of the bias extension test considered here, we have that traction boundary conditions are assigned on the surfaces Σ_3 and Σ_4. More precisely, we have that $\Sigma_{T_1} \equiv \Sigma_{T_2} = \Sigma_3 \bigcup \Sigma_4$: forces and double forces are simultaneously assigned on Σ_3 and Σ_4. More particularly, since in the Bias Extension Test Σ_3 and Σ_4 are free boundaries the assigned value of forces and double forces is the null value:

$$f = 0, \qquad \tau = 0.$$

2.2.3 Space of configurations for the bias extension test

Once that the works of external and internal actions have been given for the considered particular case, the kinematical boundary conditions must be assigned and the associated space of configurations and of admissible variations must be identified.

For the experimental set-up of the Bias Extension test shown in Fig. 2, we want to assign

- $u = 0$ and $\varphi = 0$ on Σ_1 and
- $u = u_0 = \text{const}$ and $\varphi = 0$ on Σ_2. If we want to frame this situation in the more general picture given in section 1, we have to set $\Sigma_{K_1} \equiv \Sigma_{K_2} = \Sigma_1 \bigcup \Sigma_2$ and the space of configurations $Q \times D$ for the considered micromorphic continuum subjected to a Bias Extension Test takes the particular form

$$\begin{aligned} Q &= \{u \ \mid \ u = 0 \ \text{ on } \ \Sigma_1 \quad \text{and} \quad u = u_0 = \text{const}, \ \text{ on } \ \Sigma_2\}, \\ D &= \{\varphi \ \mid \ \varphi = 0 \ \text{ on } \ \Sigma_1 \quad \text{and} \quad \varphi = 0, \ \text{ on } \ \Sigma_2\} \end{aligned} \tag{21}$$

The spaces of admissible variations that must be associated to such space of configurations are given by

$$T_u = \{\delta u \ \mid \ u + \delta u \in Q\}, \qquad T_\varphi = \{\delta\varphi \ \mid \ \varphi + \delta\varphi \in D\}. \tag{22}$$

Since both the displacement u and the angle variation φ are assigned on $\Sigma_1 \bigcup \Sigma_2$, then it must be $\delta u = 0$ and $\delta\varphi = 0$, so that the spaces of admissible variations can equivalently be written as $T_u = \{\delta u \ \mid \delta u = 0 \quad \text{on } \Sigma_1 \bigcup \Sigma_2\}$ and $T_\varphi = \{\delta\varphi \ \mid \delta\varphi = 0 \quad \text{on } \Sigma_1 \bigcup \Sigma_2\}$.

Suitably generalizing what done before, the equilibrium problem for the considered constrained micromorphic continuum subjected to a Bias Extension Test can be formulated as

Find $(u^*, \varphi^*) \in Q \times D$ *such that* $\mathcal{P}^{int}(u^*, \varphi^*, \delta u, \delta\varphi) + \mathcal{P}^{ext}(u^*, \varphi^*, \delta u, \delta\varphi) = 0 \quad$ *for any* $(\delta u, \delta\varphi) \in T_{u^*} \times T_{\varphi^*}$,

where now $\mathcal{P}^{int}$, $\mathcal{P}^{ext}$, Q, D, T_u and T_φ are given by (19), (20), (21) and (22) respectively.

The mathematical question of well-posedness of the geometrically nonlinear micromorphic approach has been discussed in [60, 58, 59]- the extension of these results to the anisotropic setting is straightforward. Some attendant results in the large strain and small strain setting, including an efficient numerical treatment and further modeling and well-posedness results can be found in [37, 46, 62, 63, 64, 61].

2.2.4 Evaluation of reaction forces and double forces

As done in subsection 1.2.1 we can ask ourselves how, in the framework of the considered constrained micromorphic model, we can calculate the reaction forces and double-forces which would be needed to produce the kinematical conditions assigned on Σ_1 and Σ_2 as well as the solution (u^*, φ^*) obtained solving the considered constrained micromorphic equilibrium problem. To do so, we proceed as in subsection 1.2.1 and we introduce a work of external forces also on the portion of the boundary $\Sigma_1 \bigcup \Sigma_2$ where kinematical boundary conditions have been assigned, so that the work of external forces takes the modified form

$$\mathcal{P}^{ext}_{II} = \int_{\Sigma_{T_1}} \langle f, \delta u\rangle \, ds + \int_{\Sigma_{T_2}} \tau \, \delta\varphi \, ds + \int_{\Sigma_{K_1}} \langle f_R, \delta u\rangle \, ds + \int_{\Sigma_{K_2}} \tau_R \, \delta\varphi ds, \tag{23}$$

where we remind that $\Sigma_{T_1} \equiv \Sigma_{T_2} = \Sigma_3 \bigcup \Sigma_4$ and that $f = 0$ and $\tau = 0$ for the considered Bias Extension Test. Moreover, $\Sigma_{K_1} \equiv \Sigma_{K_2} = \Sigma_1 \bigcup \Sigma_2$. In order to determine the reaction forces and double forces which balance the imposed displacements and angle variations on Σ_1 and Σ_2, we could pass through the use of the irreducible form of the work of internal actions, as we have explicitly shown for the first gradient case in subsection 1.2.1.

Nevertheless, since for the performed numerical simulations we only used the evaluation of volume integrals, we present here only this last method. To this aim, we write the Principle of Virtual Work for the considered particular example, evaluated in the solution $(u^*, \varphi^*, \Lambda^*)$ of the equilibrium problem, as

$$\begin{aligned}\int_B \left[-\frac{1}{2}K_{el}\left(1 - \frac{1}{\sqrt{i_4^*}}\right)\delta i_4 - \frac{1}{2}K_{el}\left(1 - \frac{1}{\sqrt{i_6^*}}\right)\delta i_6 - (K_{sh} i_8^* - \Lambda^*)\,\delta i_8 - \langle \alpha, \nabla\varphi^*\rangle \langle \alpha, \nabla\delta\varphi\rangle - \Lambda^* \, \delta\varphi \right] dv \\ - \int_B (\varphi^* - i_8^*)\delta\Lambda \, dv + \int_{\Sigma_{K_1}} \langle f_R, \delta u\rangle \, ds + \int_{\Sigma_{K_2}} \tau_R \, \delta\varphi = 0\end{aligned} \tag{24}$$

where the expression for the work of internal actions given in Eq. (18) has been used setting $i_4^* := i_4(u^*)$, $i_6^* := i_6(u^*)$, $i_8^* := i_8(u^*)$ and where we impose that this last form of the Principle of Virtual Work must be satisfied for any δu, $\delta\varphi$ and $\delta\Lambda$.

In order to calculate the reaction force, we choose particular test functions $\delta\bar{u}$, $\delta\bar{\varphi}$ and $\delta\bar{\Lambda}$ such that

1. $\delta\bar{u}$ is vanishing on Σ_1 non-vanishing and constant on Σ_2
2. $\delta\bar{u}$ is an arbitrarily assigned, non-vanishing continuous function outside Σ_{K_1}
3. $\delta\bar{\varphi} = 0$ everywhere
4. $\delta\bar{\Lambda} = 0$ everywhere.

With this choice, we can evaluate the reaction force as

$$\langle R, \delta\bar{u}\rangle = \int_B \left[\frac{1}{2}K_{el}\left(1 - \frac{1}{\sqrt{i_4^*}}\right)\delta\bar{i}_4 + \frac{1}{2}K_{el}\left(1 - \frac{1}{\sqrt{i_6^*}}\right)\delta\bar{i}_6 + (K_{sh} i_8^* - \Lambda^*)\,\delta\bar{i}_8 \right] dv \tag{25}$$

where we set $R := \int_{\Sigma_2} f_R \, ds$, $\delta\bar{i}_4 := \delta i_4(\delta\bar{u})$, $\delta\bar{i}_6 := \delta i_6(\delta\bar{u})$ and $\delta\bar{i}_8 := \delta i_4(\delta\bar{u})$. In order to evaluate the three components of the reaction force, we choose suitable test functions $\delta\bar{u}$ which are aligned with one of the

directions of the used reference system. In particular, let $\{e_i\}_{i\in\{1,2,3\}}$, be an orthonormal basis with respect to which we want to evaluate the three components $R_i = \langle R, e_i\rangle$ of the reaction force R. We choose a test function $\delta\bar{u}$ which possesses all the characteristics previously listed except that the point 1. is replaced by

- $\delta\bar{u}$ is equal to e_i on Σ_1 .

In this case the component R_i can be easily calculated according to Eq. (25).

Analogously, in order to calculate the reaction double-force, we can choose particular test functions $\delta\bar{u}$, $\delta\bar{\varphi}$ and $\delta\bar{\Lambda}$ such that

1. $\delta\bar{u} = 0$ everywhere
2. $\delta\bar{\varphi}$ is vanishing on Σ_1, non-vanishing and constant on Σ_2
3. $\delta\bar{\varphi}$ is an arbitrarily assigned, non-vanishing continuous function outside Σ_{K_1}
4. $\delta\bar{\Lambda} = 0$ everywhere.

With this choice, we can evaluate the reaction double-force as

$$\mathcal{T}\,\delta\bar{\varphi} = \int_B \left[-\langle\alpha, \nabla\varphi^*\rangle\,\langle\alpha, \nabla\delta\bar{\varphi}\rangle - \Lambda^*\,\delta\bar{\varphi}\right]\,dv, \tag{26}$$

where we set $\mathcal{T} := \int_{\Sigma_{K_2}} \tau_R\,ds$.

2.3 Numerical simulations for the constrained continuum micromorphic model

In this subsection we show the numerical simulations that we have performed in order to find numerical solutions of the equilibrium problem for an unbalanced fabric formulated as the equilibrium of a constrained micromorphic continuum subjected to a Bias Extension Test as presented in subsection 2.2. Such equilibrium problem has been implemented in COMSOL® using the weak form package in which the expression (18) for the work of internal actions can be explicitly given. The work of external actions (20) is given in COMSOL® just leaving Σ_3 and Σ_4 free which means that forces and double forces are assigned to be vanishing on the considered subsets of the boundary. Finally, the space of configurations (21) is given assigning the kinematical boundary conditions on Σ_1 and Σ_2 as explicitly established in subsection (2.1).

The numerical values used for the constitutive parameters are shown in table (2).

K_{el}	K_{sh}	α_1	α_2
0.7 MPa	21 kPa	2 kPa·m^2	0.02 kPa·m^2

Table 2: Parameters of the constrained micromorphic continuum model.

Such values have been chosen following a precise heuristic procedure that we present here

- First of all we remarked the bending stiffness α_2 of the thin yarns is very small (eventually almost vanishing), so that we choose a tentative (very small) value for such parameter
- subsequently, we choose the bending stiffness α_1 of the thick yarns in order to fit at best the experimental S-shape of the specimen (in Fig. 5 it is shown as the unbalance on the bending stiffnesses of warp and weft is responsible for the S-shape of the specimen)
- then, we tuned the value of the "sliding" parameter K_{el} which was seen to have a direct influence on the in-plane thickness of the specimen. Turning-on this parameter the height in the middle of the specimen itself starts increasing and becomes closer to the real experimental shape (see e.g. Fig. (6))
- Finally, the in-plane shear parameter K_{sh} is tuned in order to fit at best the experimental load-displacement curve (see Fig. 8).

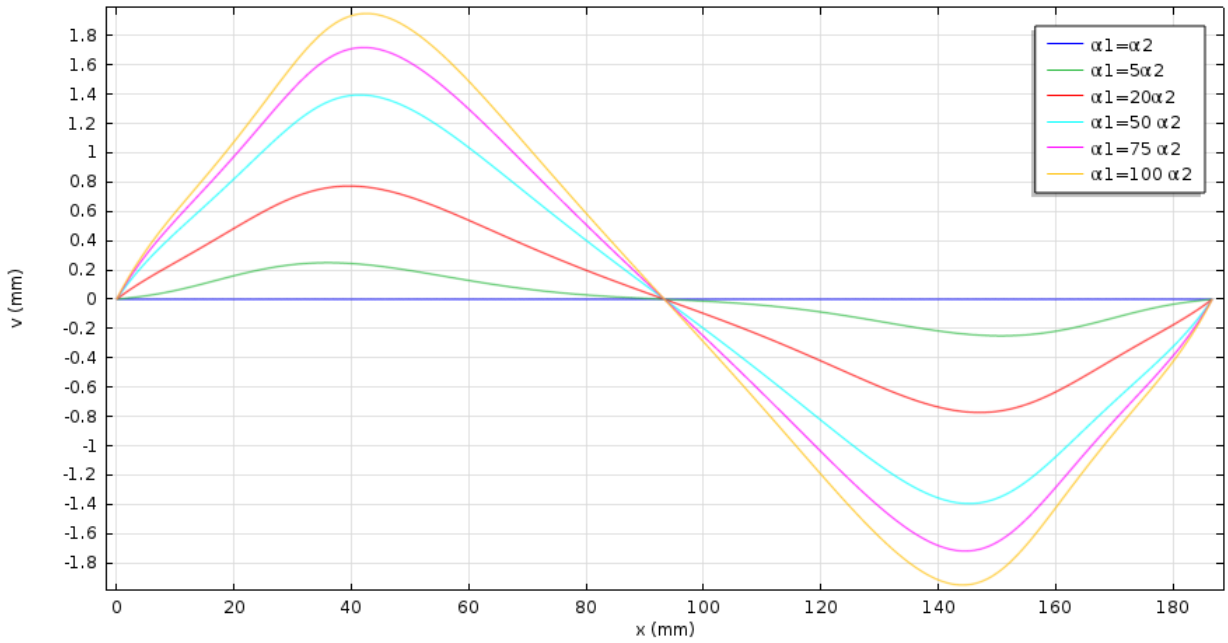

Figure 5: Vertical displacement of the mean horizontal axis for an imposed displacement of 56 mm and different values of α_1. We remark that no distortion of the specimen is present for a balanced fabric ($\alpha_1 = \alpha_2$).

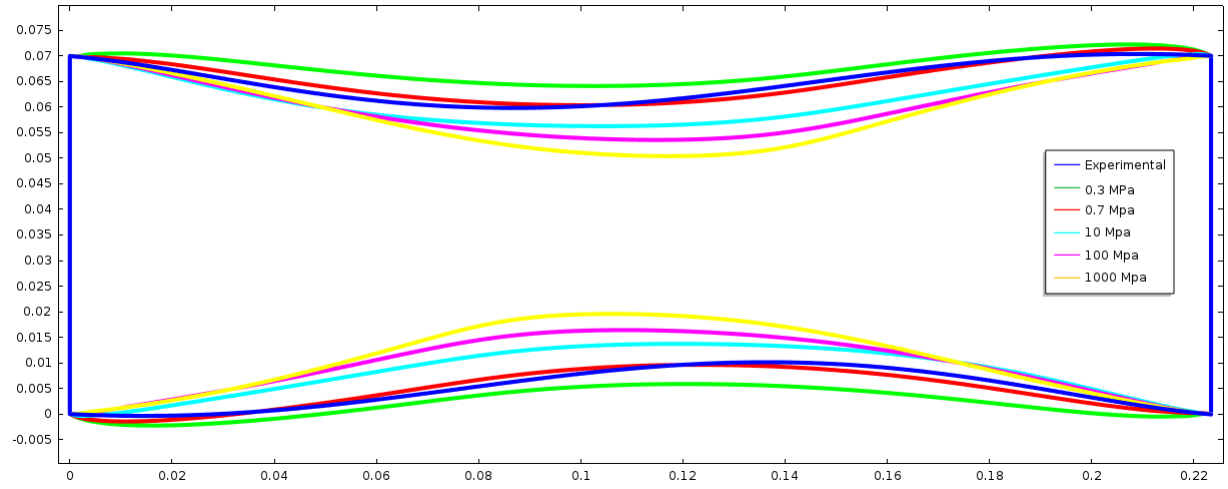

Figure 6: Deformed shape for a displacement of 37 mm and different values of K_{el}

We need to spend some extra words on the way in which the reaction force and double force have been numerically calculated.

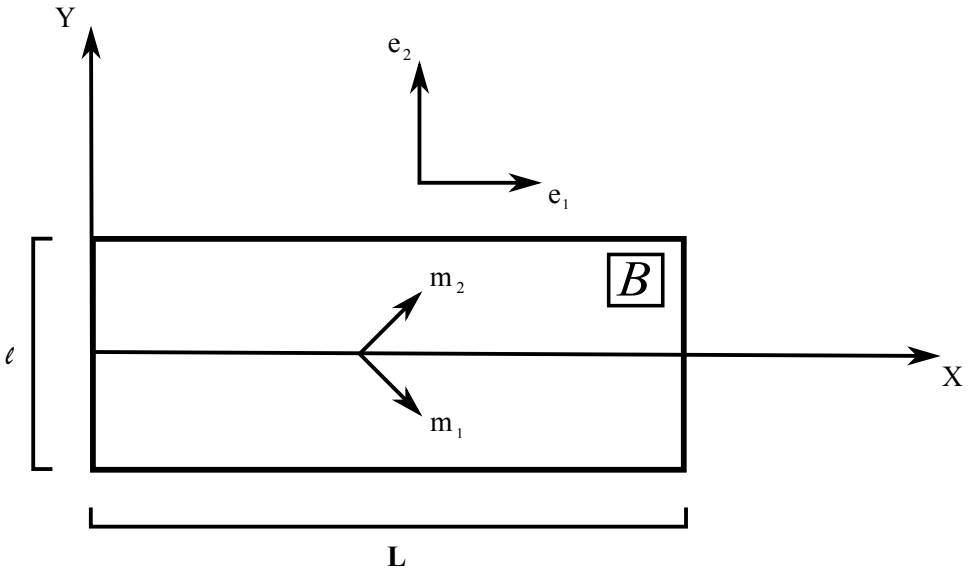

Figure 7: Definition of the global ($\{e_1, e_2\}$) and material ($\{m_1, m_2\}$) reference frames for the BET.

We followed the procedure presented in subsection 2.2.4 and, once calculated the solution $(u^*, \varphi^*, \Lambda^*)$ for each imposed displacement u_0, we calculated the horizontal component of the reaction force R with respect to an orthonormal reference frame $\{e_1, e_2\}$ chosen as in Fig. 7 by using equation (25), where we chose particular test functions $\delta\bar{u}$, $\delta\bar{\varphi}$ and $\delta\bar{\Lambda}$ such that

1. $\delta\bar{u} \cdot e_1 = \frac{X}{L}, \qquad \forall (X, Y) \in B$
2. $\delta\bar{u} \cdot e_2 = 0, \qquad \forall (X, Y) \in B$
3. $\delta\bar{\varphi} = 0, \qquad \forall (X, Y) \in B$
4. $\delta\bar{\Lambda} = 0, \qquad \forall (X, Y) \in B.$

The obtained force-displacement curve is shown in Fig. 8, where the comparison with the experimental curve and with the reaction force automatically calculated by COMSOL® are also depicted.

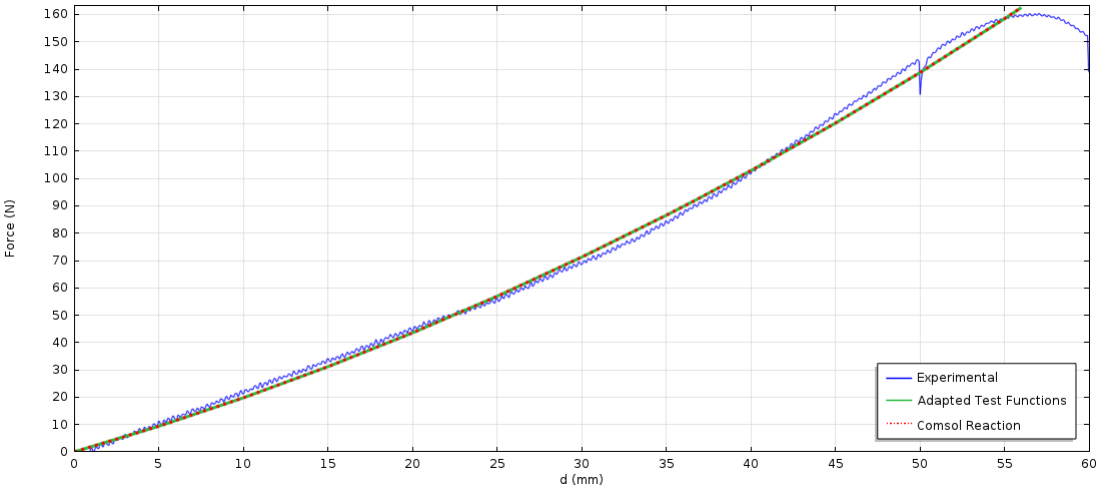

Figure 8: Load/displacement curve for the constrained micromorphic model

In figures 9 and 10 it is shown the deformed shape for two imposed displacements u_0, obtained via the numerical simulations performed to solve the considered equilibrium of the constrained micromorphic model. We remark that the following observations can be easily inferred from the performed numerical simulations:

- The macroscopic shape of the specimen is completely recovered.
- The microscopic pattern for the warp and weft is caught to a big extent. Indeed, the real behavior of the thick yarns is almost perfectly recovered, while, the thin yarns which are experimentally seen to undergo non-negligible slipping, are seen to be fictively elongated. We can affirm that where the thin yarns are seen to be elongated with respect to their initial length a slipping is taking place.
- The shear parameter is chosen to correctly fit the experimental load-displacement curve. We highlight the fact that the "force" of the introduced constrained micromorphic model is, to our understanding, the correct one to be compared to the experimental one. In fact, in our micromorphic model, we defined "force" the quantity which is dual to the virtual displacement δu. From a direct observation of the irreducible form of the work of internal forces (19), we can infer that the internal actions which balance a boundary externally applied force are directly determined by equivalent elongations, shear angle variations and microstructure-related deformation mechanisms (through the Lagrange multiplier Λ). Analogously, we can infer that the boundary internal actions (double-forces) which are dual to the angle variation $\delta\varphi$ are directly determined by the localized bending strains which occur inside the considered specimen. We state that the double-forces which are generated by the imposition of the angle between warp and weft at the two extremities of the specimen do not contribute to the "force" which is measured by the testing machine. Indeed, such angle is maintained fixed by the clamp device used during the BET and a supplementary measurement tool would be needed in order to measure such sort of couple which is generated by the clamp in order to keep the angle constant at the boundary during the test. In summary, we are reasonably assuming that the machine only senses those macro and micro deformations modes which induce macroscopic displacements (elongations, angle variations and part of the local bending), while the remaining part of the local bending energy which is localized at the micro-level is not sensed by the used machine.

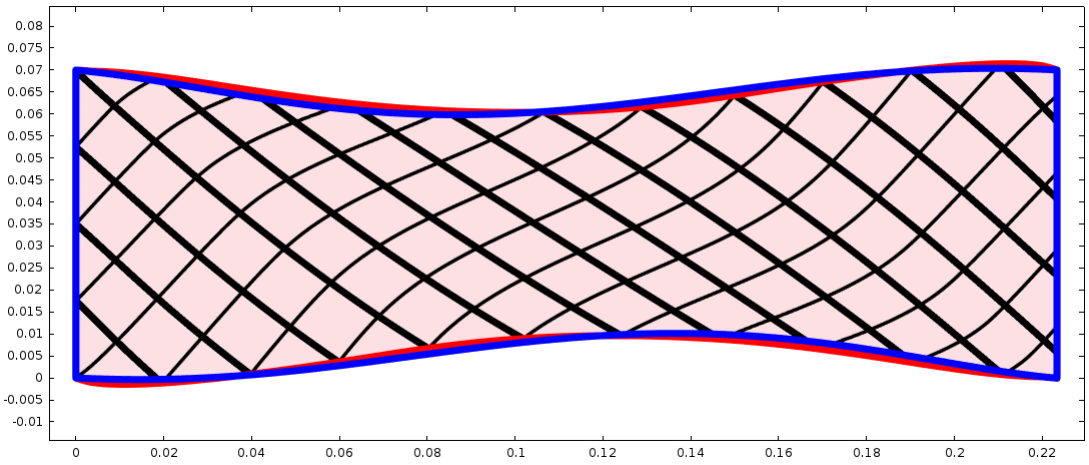

Figure 9: Deformed shape in the simulation (red with black fibers) and experimental (Blue) for a displacement of 37 mm

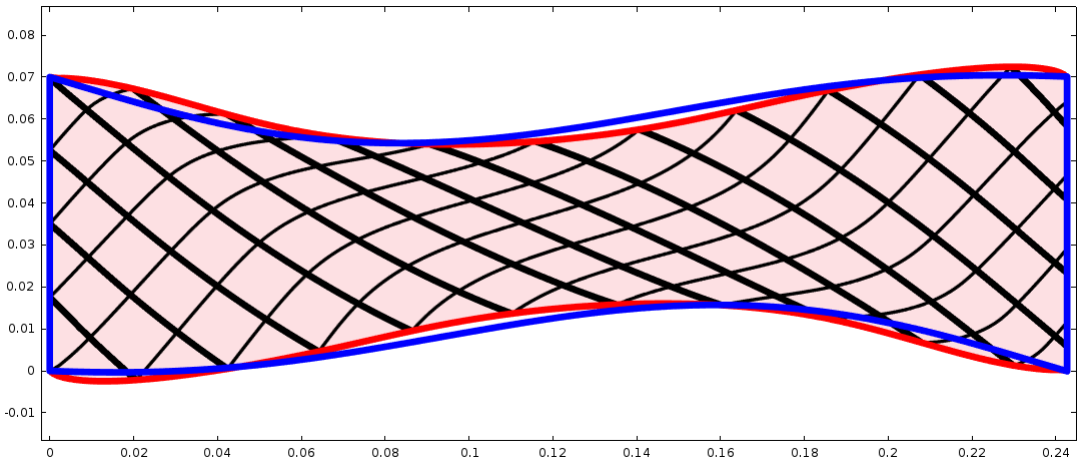

Figure 10: Deformed shape in the simulation (red with black fibers) and experimental (blue) for a displacement of 56 mm

As already pointed out, the used micromorphic model possesses a feature that the first gradient models do not posses. In particular, the reaction at the clamps is not limited to a force, but a double-force (a couple) arises which is needed to keep the angle between warp and weft constant during the test. Following the methods described in subsection 2.2.4, once calculated the solution $(u^*, \varphi^*, \Lambda^*)$ for a given imposed displacement u_0, it is possible to evaluate the reaction double-force $\mathcal{T}$ with respect to an orthonormal reference frame $\{e_1, e_2\}$ chosen as in Fig. 7 by using equation (26), where we chose particular test functions $\delta\bar{u}$, $\delta\bar{\varphi}$ and $\delta\bar{\Lambda}$ such that

1. $\delta\bar{u} \cdot e_1 = 0, \qquad \forall (X, Y) \in B$
2. $\delta\bar{u} \cdot e_2 = 0, \qquad \forall (X, Y) \in B$
3. $\delta\bar{\varphi} = \frac{X}{L}, \qquad \forall (X, Y) \in B$
4. $\delta\bar{\Lambda} = 0, \qquad \forall (X, Y) \in B.$

The results obtained are shown in figure 11 where the computed reaction double-force is also compared with the one automatically evaluated by COMSOL® .

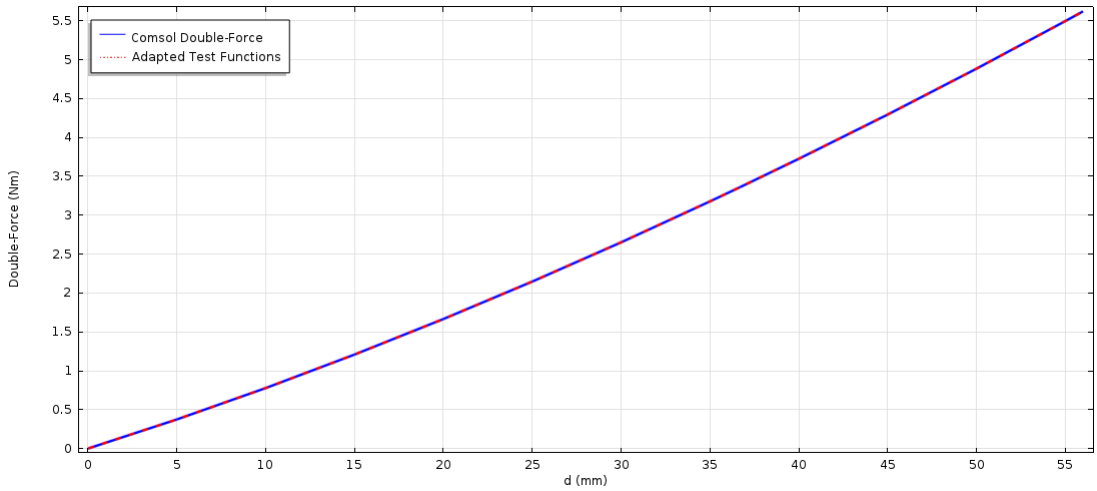

Figure 11: Double-force/displacement curve as reaction $\mathcal{T}$ dual of $\delta\varphi$.

In a material in which the shear is the main deformation mode one of the most important features to check is the angle between the fibers.

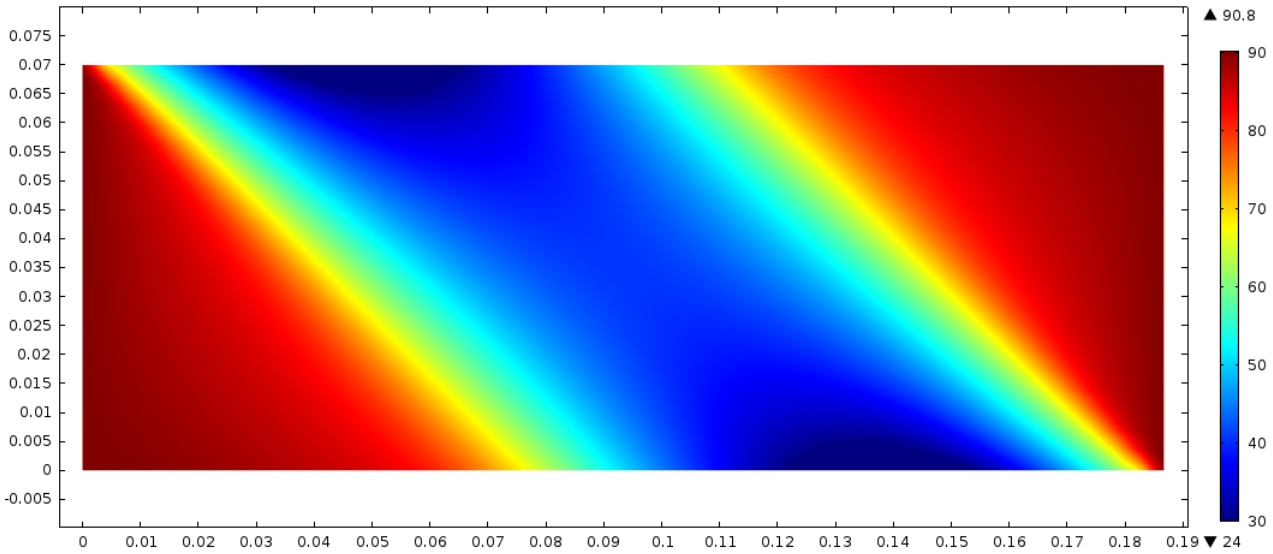

Figure 12: Angles between the fibers in the constrained micromorphic simulation for a displacement of of 56 mm

It can be noticed from Fig. 12 that no angle variation occurs in the red regions, while an important and almost constant angle variation occurs in the middle of the specimen. The transition from one value of the angle to the other one is made thanks to the creation of transition zones in which a smooth variation occurs. By direct comparison with Fig. 10 it is possible to remark that the three regions at constant shear angle individuated in Fig. 12 are determined by the fact that the thick yarns remain substantially undeformed, while the thin yarns are kinematically blocked in the standard triangular zones of the BET, while bend in the central part of the specimen. The change of direction of the thin yarns is the only one that determines the angle variation between warp a weft.

We can finally remark that the bending of the thin yarns takes place in well defined transition zones where smooth variation of the shear angle occur.

3 Discrete numerical simulations

In this section we propose to set up a suitable discrete model in which the motions of the single yarns are singularly taken into account. To do so, we decide to use Euler-Bernoulli beams with different bending rigidities which are interconnected with rotational and translational elastic springs in order to mimic at best the real connections between the yarns. The results obtained with such discrete model allow to

- explicitly account for the slipping of the yarns
- better understand the potentialities and limitations of the constrained micromorphic continuum model introduced in the previous section.

The main limitation of the discrete model that we are going to present can be found in the fact that the interactions between adjacent fibers are all considered to be elastic. If this can be considered to be reasonable to a certain extent, there are for sure some irreversible mechanisms such as friction that cannot be precisely described here and that should follow the methods presented in [35] in order to be fully taken into account. Indeed, when unloading the experimental specimen once that the BET has been performed, is not sufficient to let the specimen return in its initial configuration. This means that a certain part of the deformation is not elastic, but is due to irreversible mechanisms such as friction. Nevertheless a big amount of the imposed deformation is recovered and we can hence suppose that the discrete model which we introduce here can be thought to be a reasonable compromise between the complexity of the real microstructural motions and the simplicity of the model that one wants to introduce.

The warp and weft yarns are modeled as long Euler-Bernouilli beams disposed at 45 degrees with respect to the edges of the specimen (see Fig. 13). The connections between the two families of fibers is guaranteed

at the contact points by rotational and translational springs as the ones sketched in Fig. 14. Both beams and springs, are considered to be linear.

More particularly, the two families of yarns are modeled as beams with axial stiffness respectively $K_1 = EA_1$ and $K_2 = EA_2$, and bending stiffness respectively $K_3 = EI_1$ and $K_4 = EI_2$ where E is the Young modulus of the material constituting the yarns, A_1 and A_2 are the cross sections and I_1, I_2 the equivalent moments of inertia. In order to model the interactions between the yarns the set of points in which the two families of fibers intersect have been defined in COMSOL®. In this set of points, the interactions between the two fibers are supposed to be

- the resistance to the variation of angle between the fibers, namely the shear stiffness which are accounted for by the introduction of a set of rotational springs of stiffness K_φ
- the resistance to the slippages, described by a second set of translational springs of stiffness K_{slip} to describe the response to slippages.
- the mutual interactions between parallel fibers which are guaranteed by the weaving. Such interactions are due to the presence of the orthogonal yarns which connect the two adjacent yarns considered here. Therefore a set of springs (modeled as trusses with axial stiffness K_{inter}) has been inserted between every two couples of close interaction points belonging to two different close yarns of the same family (see Fig 14).

A possible downside of such discrete model is its difficult application for bigger specimens due to the high number of degrees of freedom needed for a proper description of the yarns response. In this optic, continuum models are preferable to discrete ones in view of the design of engineering structures.

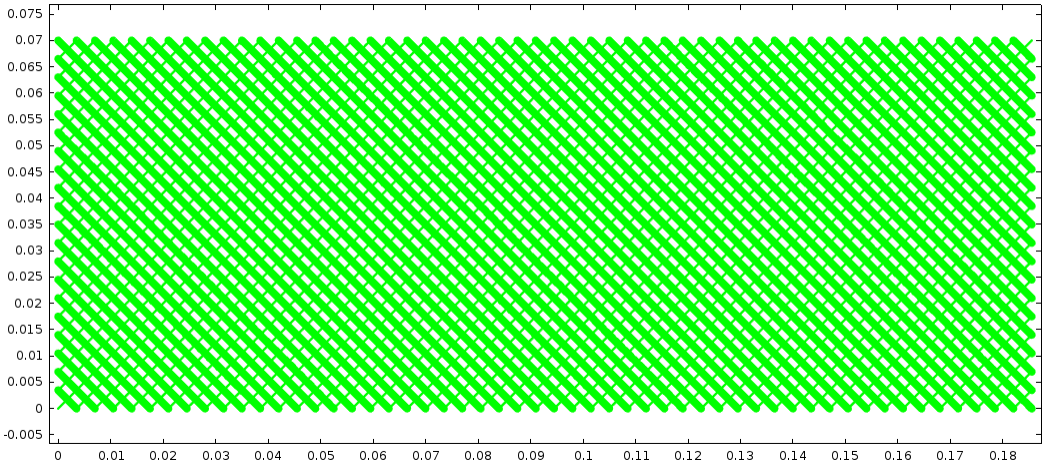

Figure 13: Geometry of the discrete model: undeformed configuration.

In order to compare the discrete model with the results of the continuous ones it was implemented in COMSOL®. In order to have a proper comparison,

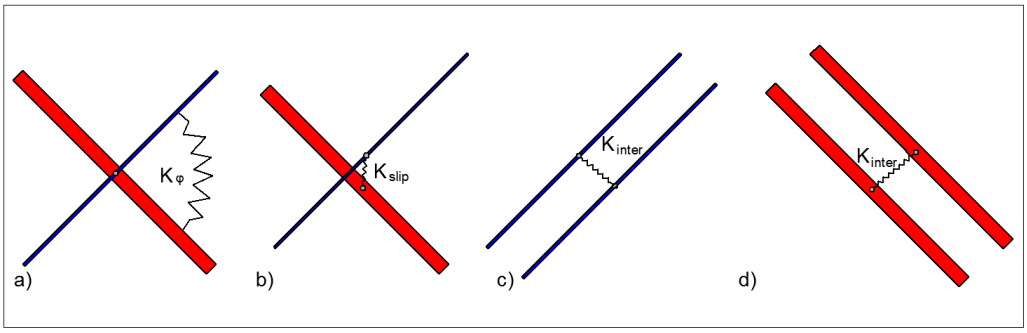

Figure 14: Schematics of the elastic interconnections between warp and weft yarns. (a) rotational spring, (b) translational spring, (c) interaction between thin yarns and (d) interaction between thick yarns.

The elastic parameters used are shown in table 3. They have been chosen in order to be reasonably compatible with yarns of small cross section area and Young moduli of carbon. The two elongation stiffnesses K_1 and K_2 have been chosen of the same of magnitude in order to underline the fact that it is indeed the difference in the bending stiffness of the two families of yarns which drives the asymmetry of the macroscopic deformation. It must be pointed out that as far as this value is high enough it does not have a big influence in the results in terms of both displacement and reactions. The parameters relative to the bending stiffness, the slipping and the interaction between two fibers of the same set were chosen via a fit of the experimental shape of the specimen. In particular the following characteristics were used to fit the different parameters: the width of the specimen in the central part, the macroscopic S-deformation, the slipping of the fibers and the distance between the fibers of the same set. The shear stiffness K_φ, was chosen in order to fit the experimental force with the reaction evaluated with the simulations.

K_1	K_2	K_3	K_4	K_φ	K_{slip}	K_{inter}
50000 N	50000 N	0.4 N·m^2	10^{-3} N·m^2	2.510^{-4}N·m	11 N/m	11 N

Table 3: Parameters of the discrete model

As done in the continuum model, in the figures 15 and 16 it is possible to see that the discrete model well describes the S-response even at different values of displacement.

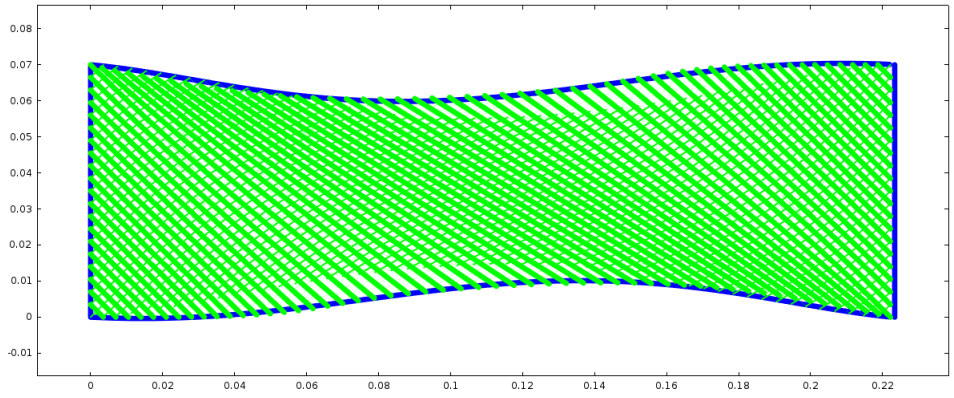

Figure 15: Deformed shape in the simulation (green) and experimental (blue) for a displacement of 37 mm

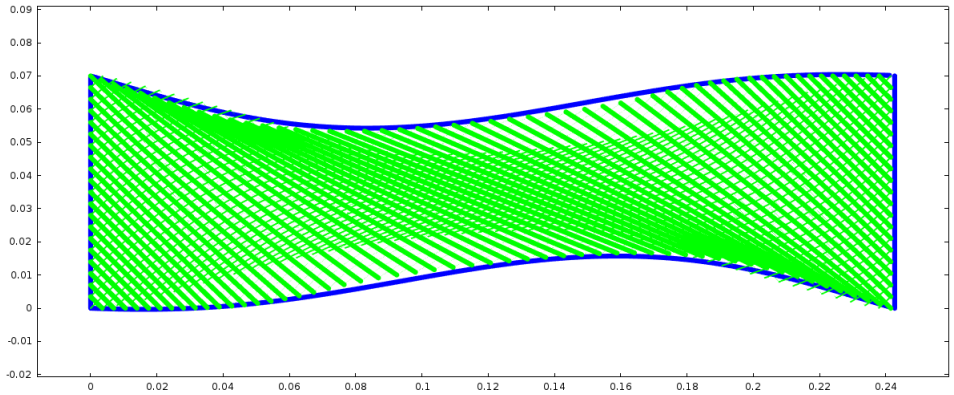

Figure 16: Deformed shape in the simulation (green) and experimental (blue) for a displacement of 56 mm

The fact that the introduced model is able to well describe the slipping between the yarns can be more precisely seen with reference to figures 17 and 18.

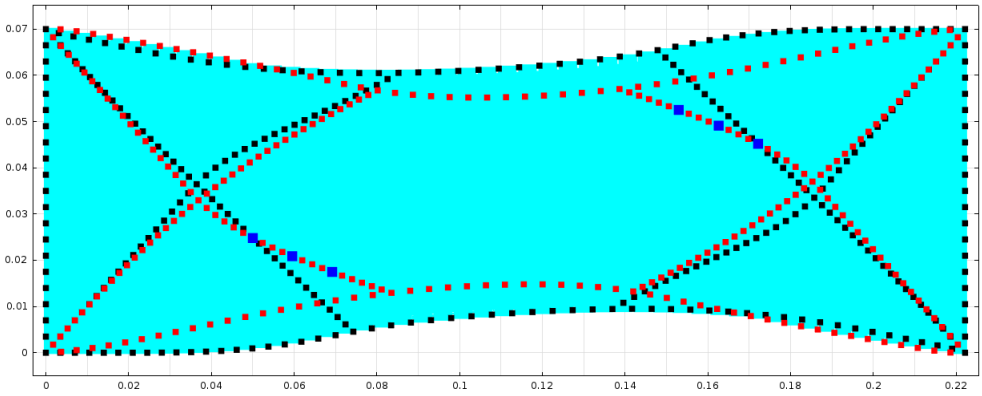

Figure 17: Deformed shape for a displacement of 56 mm and some initially superimposed points belonging to thick yarns (black) and to thin yarns (red). The highlighted blue points correspond to the experimental ones that can be observed in Fig. 18.

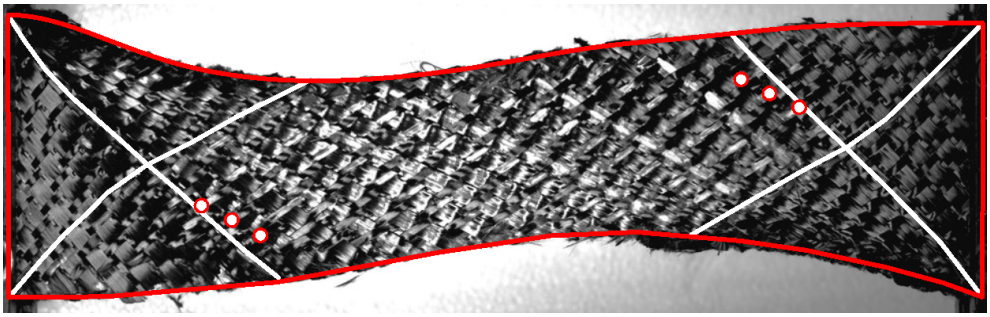

Figure 18: Deformed experimental shape: individuation of the slipping points.

In fact, the slippage of thin fibers can be recognized since

- the points of the thin fibers (red) which are initially located at the free boundaries are finally located inside the specimen.
- the blue points highlighted in Fig. 17 and belonging to the thin yarns are easily recognizable in the experimental deformed specimen shown in Fig. 18 and it can be recognized that the simulation well describes the experimental behavior, at least qualitatively.

The response of this model can be compared to the one obtained with the constrained micromorphic continuum model. Indeed the different bending stiffnesses of the two families of yarns lead to a set of straight thick fibers and a set of strongly bent thin fibers like in the continuum case. In this discrete simulation, nevertheless, the slippages of the yarns are more precisely described.

We show in Fig. 19 that, with the constitutive choice of the parameters shown in table 3, also the load-displacement curve of the discrete model results to be consistent with the experimentally obtained one, as well as with that obtained by means of the constrained micromorphic continuum model. We can notice that a slightly better fitting is recovered for the discrete model at moderate strains. A better fitting of the continuum model xould be obtained for such moderate strains if more complex hyperelastic laws would be introduced, but this falls outside the scope of the present paper.

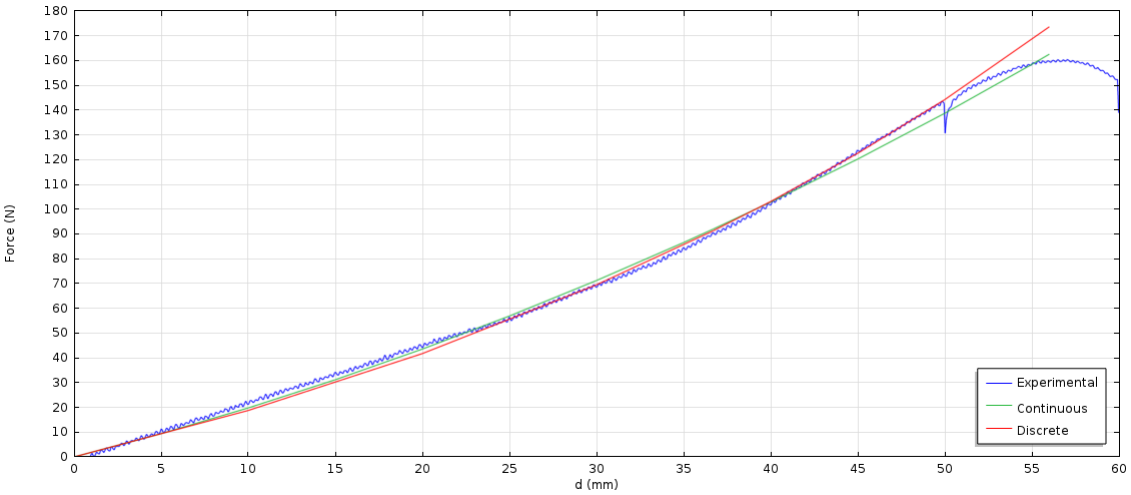

Figure 19: Load-displacement curve for the experimental, discrete and second gradient models

Finally, Fig. 20 shows the angle between warp and weft yarns as obtained with the discrete model., even in this model the angle between the set of fibers is almost a constant along the strong fibers direction while drastically changes along the think yarns. The results of both the discrete and constrained micromorphic continuum models, even with their very different natures, present the same qualitative description of the experimental behavior reconfirming the good analogy between the bending stiffness of the yarns and the second gradient effects in the continuum. This is another hint toward the importance of the insertion of a second gradient energy in a continuous models in order to fully describe the phenomenological mechanical response of the woven fabrics.

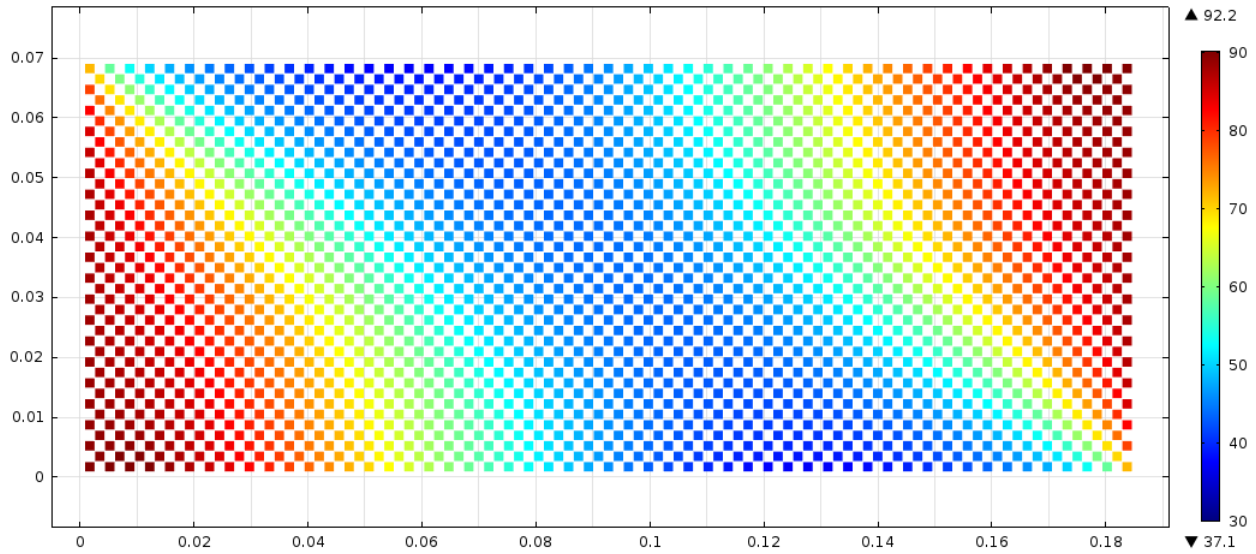

Figure 20: Angles between the fibers in the discrete simulations for a displacement of of 56 mm

Further investigations should be more systematically directed towards the quantitative analysis needed to precisely identify the macroscopic constitutive parameters in terms of the microscopic properties of the yarns. Suitable multi-scale methods as the one introduced in [56] may be generalized to be applied to the present case. Moreover, the description of the considered system at the microscopic scale may take advantage of some of the results proposed in [4, 40, 76, 73, 77, 74, 75, 83].

4 Conclusions

In this paper a continuum constrained micromorphic model and a discrete model are introduced to reproduce the Bias Extension Test on unbalanced fabrics. We show that both models are able to account for the main macroscopic and microscopic deformation mechanisms that take place during the BET up to moderate strains, namely

- the angle variation between warp and weft tows,
- the different bending stiffnesses of the two families of yarns (which is at the origin of the asymmetric macroscopic S-shape of the specimen)
- the relative slipping of the yarns.

The results obtained with the two models are satisfactory when considering small and moderate deformations so that it is conceivable to use the proposed models on more extended experimental campaigns. This would allow a more precise identification of the introduced constitutive parameters, above all for what concerns the different bending stiffnesses which are the main characteristics of fibrous composite interlocks.

Further studies should be focused on the improvement of the proposed models in the optic of more precisely describe irreversible phenomena as friction which can have a non-negligible role during the deformation of woven reinforcements.

Moreover, more extensive experimental campaigns should be carried out in order to determine which is the strain threshold until which the integrity of the material is preserved and both the continuum and discrete models can be considered to be predictive. In fact, after a given macroscopic deformation, some yarns start to be pulled out from the specimen, so that further modeling efforts intrinsically loose their interest.

Finally, the theoretical and numerical tools presented in this paper can be extended in order to treat equilibrium problems concerning 3D composite interlocks. For example, the 3 point bending test on unbalanced fabrics could be a useful way of testing and indirectly fitting new constitutive parameters related to the out-of plane different bending stiffnesses of the two families of yarns.

Acknowledgements

The authors thank CNRS for the PEPS project which assured financial support to research presented in this paper.

5 References

[1] Elias C. Aifantis. On the role of gradients in the localization of deformation and fracture. *International Journal of Engineering Science*, 30(10):1279–1299, 1992.

[2] Yamina Aimène, Emmanuelle Vidal-Sallé, Benjamin Hagège, François Sidoroff, and Philippe Boisse. A hyperelastic approach for composite reinforcement large deformation analysis. *Journal of Composite Materials*, 44(1):5–26, 2010.

[3] Jean-Jacques Alibert, Pierre Seppecher, and Francesco dell'Isola. Truss modular beams with deformation energy depending on higher displacement gradients. *Mathematics and Mechanics of Solids*, 8(1):51–73, 2003.

[4] Ali Asghar Atai and David J. Steigmann. On the nonlinear mechanics of discrete networks. *Archive of Applied mechanics*, 67(5):303–319, 1997.

[5] Daniel Balzani, Patrizio Neff, Jörg Schröder, and Gerhard A. Holzapfel. A polyconvex framework for soft biological tissues. Adjustment to experimental data. *International Journal of Solids and Structures*, 43(20):6052–6070, 2006.

[6] Jeffrey L. Bleustein. A note on the boundary conditions of Toupin's strain-gradient theory. *International Journal of Solids and Structures*, 3(6):1053–1057, 1967.

[7] Jean-Paul Boehler. Lois de comportement anisotrope des milieux continus. *Journal de Mécanique*, 17(153):70, 1978.

[8] Jean-Paul Boehler. Introduction to the invariant formulation of anisotropic constitutive equations. In *Applications of Tensor Functions in Solid Mechanics*, pages 13–30. Springer Vienna, Vienna, 1987.

[9] Philippe Boisse, A. Hakim Cherouat, Jean Claude Gelin, and Hamid Sabhi. Experimental study and finite element simulation of a glass fiber fabric shaping process. *Polymer composites*, 16(1):83–95, 1995.

[10] Jian Cao, Remko Akkerman, Philippe Boisse, Julie Chen, H. S. Cheng, E. F. de Graaf, J. L. Gorczyca, Philip Harrison, Gilles Hivet, Jérôme Launay, Wonoh Lee, L. Liu, Stepan V. Lomov, Andrew C. Long, Emmanuel de Luycker, Fabrice Morestin, J. Padvoiskis, Xiongqi Peng, James Sherwood, T. Stoilova, Xiaoming M. Tao, I. Verpoest, A. Willems, Joram Wiggers, T. X. Yu, and B. Zhu. Characterization of mechanical behavior of woven fabrics: Experimental methods and benchmark results. *Composites Part A: Applied Science and Manufacturing*, 39(6):1037–1053, 2008.

[11] P. Casal. La théorie du second gradient et la capillarité. *Comptes Rendus de l'Académie des Sciences - Series A*, 274:1571–1574, 1972.

[12] Adrien Charmetant, Jean Guillaume Orliac, Emmanuelle Vidal-Sallé, and Philippe Boisse. Hyperelastic model for large deformation analyses of 3D interlock composite preforms. *Composites Science and Technology*, 72(12):1352–1360, 2012.

[13] Adrien Charmetant, Emmanuelle Vidal-Sallé, and Philippe Boisse. Hyperelastic modelling for mesoscopic analyses of composite reinforcements. *Composites Science and Technology*, 71(14):1623–1631, 2011.

[14] Eugène Cosserat and François Cosserat. *Théorie des corps déformables (engl. translation by D. Delphenich 2007, pdf available at http://www.uni-due.de/%7ehm0014/Cosserat_files/Cosserat09_eng.pdf)*. 1909.

[15] Massimo Cuomo and M. Fagone. Finite deformation non-isotropic elasto-plasticity with evolving structural tensors. A framework. *Nuovo Cimento della Societa Italiana di Fisica C*, 32(1):55–72, 2009.

[16] Pierre-Gilles de Gennes. Some effects of long range forces on interfacial phenomena. *Journal de Physique Lettres*, 42(16):377–379, 1981.

[17] Francesco dell'Isola, Henri Gouin, and Giacomo Rotoli. Nucleation of spherical shell-like interfaces by second gradient theory: numerical simulations. *European Journal of Mechanics - B/Fluids*, 15(4):545–568, 1996.

[18] Francesco dell'Isola, Henri Gouin, and Pierre Seppecher. Radius and surface tension of microscopic bubbles by second gradient theory. *Comptes Rendus de l'Académie des Sciences - Series IIB - Mechanics-Physics-Astronomy*, 320:5, 1995.

[19] Francesco dell'Isola, Massimo Guarascio, and Kolumban Hutter. A variational approach for the deformation of a saturated porous solid. A second-gradient theory extending Terzaghi's effective stress principle. *Archive Of Applied Mechanics*, 70(5):323–337, 2000.

[20] Francesco dell'Isola, Angela Madeo, and Luca Placidi. Linear plane wave propagation and normal transmission and reflection at discontinuity surfaces in second gradient 3D continua. *Zeitschrift für Angewandte Mathematik und Mechanik*, 92(1):52–71, 2012.

[21] Francesco dell'Isola and Giacomo Rotoli. Validity of Laplace formula and dependence of surface tension on curvature in second gradient fluids. *Mechanics Research Communications*, 22(5):485–490, 1995.

[22] Francesco dell'Isola, Giulio Sciarra, and Stefano Vidoli. Generalized Hooke's law for isotropic second gradient materials. *Proceedings of the Royal Society A: Mathematical, Physical and Engineering Sciences*, 465(2107):2177–2196, 2009.

[23] Francesco dell'Isola and Pierre Seppecher. The relationship between edge contact forces , double forces and interstitial working allowed by the principle of virtual power. *Comptes Rendus de l'Académie des Sciences - Series IIB - Mechanics-Physics-Astronomy*, 3:43–48, 1995.

[24] Francesco dell'Isola and Pierre Seppecher. Edge contact forces and quasi-balanced power. *Meccanica*, 32(1):33–52, 1997.

[25] Francesco dell'Isola, Pierre Seppecher, and Angela Madeo. How contact interactions may depend on the shape of Cauchy cuts in Nth gradient continua: Approach "À la D'Alembert". *Zeitschrift für Angewandte Mathematik und Physik*, 63(6):1119–1141, 2012.

[26] Francesco dell'Isola and David J. Steigmann. A two-dimensional gradient-elasticity theory for woven fabrics. *Journal of Elasticity*, 118(1):113–125, 2015.

[27] J. P. Dumont, Pierre Ladeveze, M. Poss, and Yves Remond. Damage mechanics for 3-D composites. *Composite Structures*, 8(2):119–141, 1987.

[28] Victor A. Eremeyev. Acceleration waves in micropolar elastic media. *Doklady Physics*, 50(4):204–206, 2005.

[29] Victor A. Eremeyev, Leonid P. Lebedev, and Holm Altenbach. *Foundations of micropolar mechanics*. Springer Berlin Heidelberg, 2013.

[30] Ahmed Cemal Eringen. *Microcontinuum field theories*. Springer-Verlag, New York, 1999.

[31] Manuel Ferretti, Angela Madeo, Francesco dell'Isola, and Philippe Boisse. Modeling the onset of shear boundary layers in fibrous composite reinforcements by second-gradient theory. *Zeitschrift für Angewandte Mathematik und Physik*, 65(3):587–612, 2014.

[32] Samuel Forest. Micromorphic approach for gradient elasticity, viscoplasticity, and damage. *Journal of Engineering Mechanics*, 135(3):117–131, 2009.

[33] Samuel Forest and Elias C. Aifantis. Some links between recent gradient thermo-elasto-plasticity theories and the thermomechanics of generalized continua. *International Journal of Solids and Structures*, 47(25-26):3367–3376, 2010.

[34] Samuel Forest and Rainer Sievert. Nonlinear microstrain theories. *International Journal of Solids and Structures*, 43(24):7224–7245, 2006.

[35] Sébastien Gatouillat, Andrea Bareggi, Emmanuelle Vidal-Sallé, and Philippe Boisse. Meso modelling for composite preform shaping - Simulation of the loss of cohesion of the woven fibre network. *Composites Part A: Applied Science and Manufacturing*, 54:135–144, 2013.

[36] Paul Germain. The method of virtual power in continuum mechanics. Part 2: Microstructure. *SIAM Journal on Applied Mathematics*, 25(3):556–575, 1973.

[37] Ionel-Dumitrel Ghiba, Patrizio Neff, Angela Madeo, Luca Placidi, and Giuseppe Rosi. The relaxed linear micromorphic continuum: existence, uniqueness and continuous dependence in dynamics. *Mathematics and Mechanics of Solids*, 20(10):1171–1197, 2014.

[38] Albert Edward Green and Ronald S. Rivlin. Multipolar continuum mechanics. *Archive for Rational Mechanics and Analysis*, 17(2):113–147, 1964.

[39] Philip Harrison, Michael J. Clifford, and Andrew C. Long. Shear characterisation of viscous woven textile composites: A comparison between picture frame and bias extension experiments. *Composites Science and Technology*, 64(10-11):1453–1465, 2004.

[40] Eliza M. Haseganu and David J. Steigmann. Equilibrium analysis of finitely deformed elastic networks. *Computational Mechanics*, 17(6):359–373, 1996.

[41] Gerhard A. Holzapfel. *Nonlinear solid mechanics*. John Wiley & Sons, 2000.

[42] Gerhard A. Holzapfel, Thomas C. Gasser, and Ray W. Ogden. A new constitutive framework for arterial wall mechanics and a comparative study of material models. *Journal of Elasticity*, 61(1-3):1–48, 2000.

[43] Mikhail Itskov. On the theory of fourth-order tensors and their applications in computational mechanics. *Computer Methods in Applied Mechanics and Engineering*, 189(2):419–438, 2000.

[44] Mikhail Itskov. *Tensor Algebra and Tensor Analysis for Engineers*. Mathematical Engineering. Springer International Publishing, Cham, 2007.

[45] Mikhail Itskov and Nuri Aksel. A class of orthotropic and transversely isotropic hyperelastic constitutive models based on a polyconvex strain energy function. *International Journal of Solids and Structures*, 41(14):3833–3848, 2004.

[46] Axel Klawonn, Patrizio Neff, Oliver Rheinbach, and Stefanie Vanis. FETI-DP domain decomposition methods for elasticity with structural changes: P -elasticity. *ESAIM: Mathematical Modelling and Numerical Analysis*, 45(3):563–602, 2011.

[47] Wonoh Lee, J. Padvoiskis, Jian Cao, Emmanuel de Luycker, Philippe Boisse, Fabrice Morestin, J. Chen, and James Sherwood. Bias-extension of woven composite fabrics. *International Journal of Material Forming*, 1(SUPPL. 1):895–898, 2008.

[48] Angela Madeo, Francesco dell'Isola, Nicoletta Ianiro, and Giulio Sciarra. A variational deduction of second gradient poroelasticity II: An application to the consolidation problem. *Journal of Mechanics of Materials and Structures*, 3(4):607–625, 2008.

[49] Angela Madeo, Irini Djeran-Maigre, Giuseppe Rosi, and Claire Silvani. The effect of fluid streams in porous media on acoustic compression wave propagation, transmission, and reflection. *Continuum Mechanics and Thermodynamics*, 25(2-4):173–196, 2013.

[50] Angela Madeo, Ionel-Dumitrel Ghiba, Patrizio Neff, and Ingo Münch. A new view on boundary conditions in the Grioli–Koiter–Mindlin–Toupin indeterminate couple stress model. *European Journal of Mechanics - A/Solids*, 59:294–322, 2016.

[51] Jerrold E. Marsden, Thomas J. R. Hughes, and D. E. Carlson. *Mathematical Foundations of Elasticity*, volume 51. 1984.

[52] Amin Mikdam, Ahmed Makradi, Said Ahzi, Hamid Garmestani, Dongsheng S. Li, and Yves Remond. Effective conductivity in isotropic heterogeneous media using a strong-contrast statistical continuum theory. *Journal of the Mechanics and Physics of Solids*, 57(1):76–86, 2009.

[53] Amin Mikdam, Ahmed Makradi, Said Ahzi, Hamid Garmestani, Dongsheng S. Li, and Yves Remond. Statistical continuum theory for the effective conductivity of fiber filled polymer composites: Effect of orientation distribution and aspect ratio. *Composites Science and Technology*, 70(3):510–517, 2010.

[54] Raymond David Mindlin. Micro-structure in linear elasticity. *Archive for Rational Mechanics and Analysis*, 16(1):51–78, 1964.

[55] Raymond David Mindlin and N. N. Eshel. On first strain-gradient theories in linear elasticity. *International Journal of Solids and Structures*, 4(1):109–124, 1968.

[56] Ben Nadler, Panayiotis Papadopoulos, and David J. Steigmann. Multiscale constitutive modeling and numerical simulation of fabric material. *International Journal of Solids and Structures*, 43(2):206–221, 2006.

[57] Ben Nadler and David J. Steigmann. A model for frictional slip in woven fabrics. *Comptes Rendus - Mecanique*, 331(12):797–804, 2003.

[58] Patrizio Neff. Existence of minimizers for a finite-strain micromorphic elastic solid. *Proceedings of the Royal Society of Edinburgh: Section A Mathematics*, 136(05):997, 2006.

[59] Patrizio Neff. Existence of minimizers in nonlinear elastostatics of micromorphic solids. In *Encyclopedia of Thermal Stresses*, pages 1475–1485. Springer, 2014.

[60] Patrizio Neff and Samuel Forest. A geometrically exact micromorphic model for elastic metallic foams accounting for affine microstructure. Modelling, existence of minimizers, identification of moduli and computational results. *Journal of Elasticity*, 87(2-3):239–276, 2007.

[61] Patrizio Neff, Ionel-Dumitrel Ghiba, Markus Lazar, and Angela Madeo. The relaxed linear micromorphic continuum: well-posedness of the static problem and relations to the gauge theory of dislocations. *The Quarterly Journal of Mechanics and Applied Mathematics*, 68(1):53–84, 2015.

[62] Patrizio Neff, Ionel-Dumitrel Ghiba, Angela Madeo, Luca Placidi, and Giuseppe Rosi. A unifying perspective: the relaxed linear micromorphic continuum. *Continuum Mechanics and Thermodynamics*, 26(5):639–681, 2014.

[63] Patrizio Neff, Jena Jeong, Ingo Münch, and Hamidréza Ramézani. Mean field modeling of isotropic random Cauchy elasticity versus microstretch elasticity. *Zeitschrift für angewandte Mathematik und Physik*, 60(3):479–497, 2009.

[64] Patrizio Neff, Jena Jeong, and Hamidréza Ramézani. Subgrid interaction and micro-randomness - Novel invariance requirements in infinitesimal gradient elasticity. *International Journal of Solids and Structures*, 46(25-26):4261–4276, 2009.

[65] Ray W. Ogden. *Non-linear elastic deformations*, volume 1. 1984.

[66] Ray W. Ogden. Nonlinear Elasticity, Anisotropy, Material Stability and Residual Stresses in Soft Tissue. In *Biomechanics of Soft Tissue in Cardiovascular Systems*, volume 108, pages 65–108. Springer-Verlag, Vienna, 2003.

[67] Victor G. Oshmyan, Stanislav A. Patlazhan, and Yves Remond. Principles of structural-mechanical modeling of polymers and composites. *Polymer Science Series A*, 48(9):1004–1013, 2006.

[68] Xiongqi Peng, Jian Cao, J. Chen, P. Xue, D. S. Lussier, and L. Liu. Experimental and numerical analysis on normalization of picture frame tests for composite materials. *Composites Science and Technology*, 64(1):11–21, 2004.

[69] Catherine Pideri and Pierre Seppecher. A second gradient material resulting from the homogenization of an heterogeneous linear elastic medium. *Continuum Mechanics and Thermodynamics*, 9(5):241–257, 1997.

[70] Gabbro Piola. Memoria intorno alle equazioni fondamentali del movimento di corpi qualsivogliono considerati secondo la naturale loro forma e costituzione. *Modena, Tipi del R.D. Camera*, 1846.

[71] Luca Placidi, Giuseppe Rosi, Ivan Giorgio, and Angela Madeo. Reflection and transmission of plane waves at surfaces carrying material properties and embedded in second-gradient materials. *Mathematics and Mechanics of Solids*, 19(5):555–578, 2014.

[72] Annie Raoult. Symmetry groups in nonlinear elasticity: an exercise in vintage mathematics. *Communications on Pure and Applied Analysis*, 8(1):435–456, 2008.

[73] Antonio Rinaldi. Rational Damage Model of 2D Disordered Brittle Lattices Under Uniaxial Loadings. *International Journal of Damage Mechanics*, 18(3):233–257, 2008.

[74] Antonio Rinaldi. Statistical model with two order parameters for ductile and soft fiber bundles in nanoscience and biomaterials. *Physical Review E*, 83(4):046126, 2011.

[75] Antonio Rinaldi. Bottom-up modeling of damage in heterogeneous quasi-brittle solids. *Continuum Mechanics and Thermodynamics*, 25(2-4):359–373, 2013.

[76] Antonio Rinaldi, Dusan Krajcinovic, Pedro Peralta, and Ying-Cheng Lai. Lattice models of polycrystalline microstructures: A quantitative approach. *Mechanics of Materials*, 40(1-2):17–36, 2008.

[77] Antonio Rinaldi and Ying-Cheng Lai. Statistical damage theory of 2D lattices: Energetics and physical foundations of damage parameter. *International Journal of Plasticity*, 23(10-11):1796–1825, 2007.

[78] Giuseppe Rosi, Angela Madeo, and Jean-Louis Guyader. Switch between fast and slow Biot compression waves induced by "second gradient microstructure" at material discontinuity surfaces in porous media. *International Journal of Solids and Structures*, 50(10):1721–1746, 2013.

[79] Jörg Schröder, Patrizio Neff, and Daniel Balzani. A variational approach for materially stable anisotropic hyperelasticity. *International Journal of Solids and Structures*, 42(15):4352–4371, 2005.

[80] Giulio Sciarra, Francesco dell'Isola, and Olivier Coussy. Second gradient poromechanics. *International Journal of Solids and Structures*, 44(20):6607–6629, 2007.

[81] Giulio Sciarra, Francesco dell'Isola, Nicoletta Ianiro, and Angela Madeo. A variational deduction of second gradient poroelasticity I: general theory. *Journal of Mechanics of Materials and Structures*, 3(3):507–526, may 2008.

[82] Pierre Seppecher, Jean-Jacques Alibert, and Francesco dell'Isola. Linear elastic trusses leading to continua with exotic mechanical interactions. *Journal of Physics: Conference Series*, 319(1):012018, 2011.

[83] David J. Steigmann. Equilibrium of prestressed networks. *IMA Journal of Applied Mathematics*, 48(2):195–215, 1992.

[84] David J. Steigmann. Invariants of the stretch tensors and their application to finite elasticity theory. *Mathematics and Mechanics of Solids*, 7(4):393–404, 2002.

[85] David J. Steigmann. Frame-invariant polyconvex strain-energy functions for some anisotropic solids. *Mathematics and Mechanics of Solids*, 8(5):497–506, 2003.

[86] Richard A. Toupin. Theories of elasticity with couple-stress. *Archive for Rational Mechanics and Analysis*, 17(2):85–112, 1964.

[87] Nicolas Triantafyllidis and Elias C. Aifantis. A gradient approach to localization of deformation. I. Hyperelastic materials. *Journal of Elasticity*, 16(3):225–237, 1986.

Appendix A: Alternative numerical implementation of the constrained micromorphic model: penalty method

In this subsection, we briefly mention a method that can be used in order to numerically implement a constrained micromorphic model as an alternative to the method of Lagrange multipliers described in subsection 2.2.1. It is known as "penalty method" and consists in implementing a strain energy density which takes the form

$$W(i_4, i_6, i_8, \varphi, \nabla\varphi) = W_I(i_4, i_6, i_8) + W_{II}(\nabla\varphi) + W_{coupling}(i_8, \varphi), \tag{27}$$

where W_I and W_{II} are given in Eqs. 14 and 15 respectively, while the coupling energy takes the form

$$W_{coupling}(i_8, \varphi) = \frac{K}{2}(\varphi - i_8)^2,$$

where K is a constant that may ideally tend to infinity. Indeed, in order to guarantee the boundedness of the strain energy density, it follows that φ must necessarily tend to i_8. We numerically implemented such penalty method in order to test the correct convergence of our equilibrium problem formulated with the Lagrange multipliers. Being K constant, the considered virtual variations are only δu and $\delta\varphi$ and, moreover, the constant K must be chosen sufficiently large in order to guarantee numerical convergence of the solution. This last feature can be easily tested by controlling that the solution does not change when increasing the value of K (see Fig. 21). The constitutive parameters remain the same as the ones used in the numerical simulation with the Lagrange multiplier (see table 2). It is possible to notice that, suitably increasing the value of K the model converges and the limit corresponds to the solution obtained with constrained micromorphic simulation with Lagrange multipliers (see also Fig. 5).

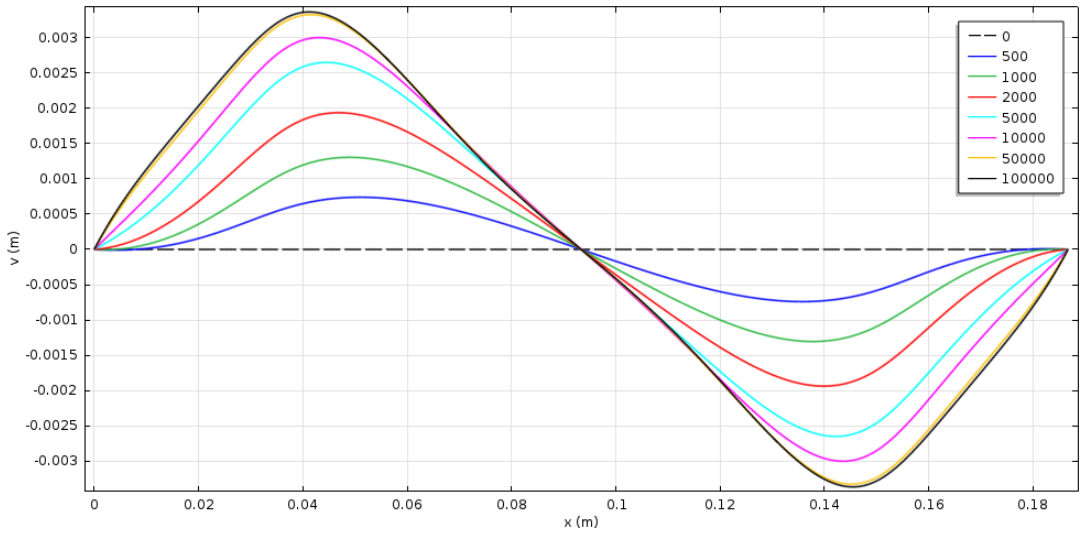

Figure 21: Vertical displacement of the mean axis for a displacement of 56 mm and different values of K

This penalty method can be seen as a useful tool for the easy implementation of constrained micromorphic models due to their high numerical stability.